Journal of Chromatography Open 6 (2024) 100147

Contents lists available at ScienceDirect

Journal of Chromatography Open

journal homepage: www.elsevier.com/locate/jcoa

Enantioseparation of organometallic compounds and metal complexes by liquid chromatographic techniques. A review

Barbara Sechi [a], Sergio Cossu [b], Paola Peluso [a,*]

[a] Istituto di Chimica Biomolecolare ICB, CNR, Sede secondaria di Sassari, Traversa La Crucca 3, I-07100 Li Punti - Sassari, Italy
[b] Dipartimento di Scienze Molecolari e Nanosistemi DSMN, Università Ca' Foscari Venezia, Via Torino 155, I-30172 Mestre Venezia, Italy

ARTICLE INFO

Keywords:
Chiral stationary phases
Enantioseparation
High-performance liquid-chromatography
Polysaccharide-based chiral selectors
Transition metal complexes

ABSTRACT

Chiral organometallic compounds and metal complexes, and more recently metal clusters, have attracted great interest for applications in chemical, biological, medical, and material sciences. In these fields, liquid chromatography has been widely used for fast chiral analysis to determine the enantiomeric purity of metal-containing chiral compounds prepared by asymmetric synthesis, for quality control of commercial chiral metal catalysts, for accessing enantioenriched or pure enantiomers of metal complexes for various applications, and often as test probe analytes for screening the enantioseparation capability of newly developed chiral columns and chromatographic systems. With the aim to show what was done in this field as a useful guide for new applications, in this review the evolution of methods and approaches used to separate the enantiomers of chiral metal-containing compounds is described, showing how this field have been changed over time, from the 1970s until most recent studies. For this purpose, representative applications of enantioselective liquid chromatography for the enantioseparation of chiral organometallic compounds and metal complexes will be presented and discussed, indicating chiral columns, mobile phases, and chromatographic conditions which have been used to obtain successful enantioseparations in this field.

1. Introduction

Over time, organometallic compounds, metal complexes, and metal clusters attracted great interest due to their versatile and modular structure. Many such compounds are now essential as catalysts, and metal-organic compounds also proved to be essential to life (methylcobalamin, hemoglobin, hemocyanin, dimethylmercury, many enzymes, cofactors, etc.). More than others, transition metal complexes were shown to play a pivotal role in medicinal biochemistry, contributing to the treatment of various human diseases [1]. Metal complexes are designed and prepared through the coordination of metallic elements with ligands via coordinate covalent bonds. Geometry and properties of the metal complex can be finely modulated through the proper selection of metal and ligand based on their stereoelectronic properties [2,3]. In most cases, the metallic element is a transition metal, belonging to the d-block (3d, 4d, and 5d series) and f-block (lanthanides and actinides) elements within the periodic table. Furthermore, different species like simple ions, molecules, or chelating groups can be used to obtain metal complexes, which function as Lewis bases forming coordinative covalent bonds with the metallic centre, acting as a Lewis acid.

In chiral metal-containing compounds, chirality may be introduced into the metal coordination sphere by using chiral ligands containing chiral centre, axis, or plane as stereogenic elements [4]. Moreover, chirality-at-metal can be observed in some transition metal complexes, even in the presence of achiral ligands, showing a suitable arrangement of the coordination sphere around the metal centre [5]. In this case, Δ and Λ enantiomers of chiral-at-metal complexes can be identified [4,5].

The origins of the liquid chromatography (LC) enantioseparation of metal-containing chiral compounds date to the decades 1950s–1970s, when diastereomeric crystallizations and the first chromatographic enantioseparations were developed for the purpose. At that time, racemic metal complex ions were usually combined with suitable optically active counter ions to form diastereomeric salts, through which the separation of the enantiomers were achieved. In 1959, Thomson reported the resolution of the first (planar) chiral ferrocene derivative, i.e. ferrocenocyclohexenone (**1**) (Fig. 1), by diastereomeric crystallization [6]. In parallel, enantioselective adsorption was obtained for chiral metal complexes by using optically active adsorbents like starch [7] and D-lactose [8].

In the 1960s, the first use of LC for the separation of organometallic

* Corresponding author.
E-mail address: paola.peluso@cnr.it (P. Peluso).

https://doi.org/10.1016/j.jcoa.2024.100147
Received 12 May 2024; Received in revised form 20 June 2024; Accepted 22 June 2024
Available online 24 June 2024

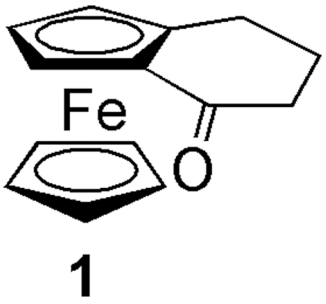

Fig. 1. Structure of planar chiral ferrocene 1.

species was reported by Veening *et al.*, who separated four arene tricarbonylchromium complexes with isooctane as mobile phase [9]. In these years, the first enantioseparations of chiral metal complexes through electromigration techniques were also performed [4]. It is worth mentioning that, over time, electromigration techniques were also used for the enantioseparation of organometallic compounds and metal complexes. The topic was reviewed very recently [4], thus applications of electromigration techniques in this field were not included in the present review.

In 1970, the first chromatographic resolution of a ferrocene derivative was reported by Schlögl, who enantioseparated chiral ferrocene **1** on acetylated cellulose under medium pressure conditions [10]. Later, Yoneda and Yoshizawa resolved the enantiomers of the [Co(β-alanine)$_3$] chiral-at-metal complex with a home-made Sephadex column using sodium *d*-tartrate as chiral selector and the mobile phase 30 % aqueous ethanol (EtOH) [11]. The fractions corresponding to the two peak maxima showed circular dichroism spectra of opposite sign, this evidence proving the complete resolution of the racemic mixture (Fig. 2). It is worth mentioning that with an eluent not containing the chiral selector as mobile phase additive, the complex was eluted as a single band. This confirmed that the chiral selector, not the Sephadex surface, promoted the enantiodifferentiation.

In 1985, Armstrong *et al.* reported a study on the LC enantioseparation of 15 enantiomeric derivatives of ferrocene (**2-14**), ruthenocene (**15**), and osmocene (**16**) on a β-cyclodextrin (CD)-based chiral column by using methanol (MeOH)/water mixtures as mobile phases (Table 1) [12]. Among all compounds, ten enantiomeric pairs (**2-4, 6-10, 15**, and **16**) were baseline or nearly baseline resolved, whereas the enantiomeric separation of amine-containing ferrocene derivatives (**12-14**) showed the poorest resolution. The authors observed that the poor resolution was not the result of poor selectivity (α) but, rather, of the extensive band broadening of these compounds under the given conditions. As justification of this phenomenon, it was thought that the extensive band broadening was caused by a kinetically limiting step involving hydrogen bonding of the amine group. Only the enantiomers of **5** and **11** were not

Table 1
Structures and retention data for several metallocene enantiomers separated on a 25-cm β-cyclodextrin column [12].

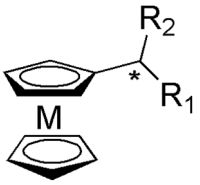

Metallocene	M	R_1	R_2	α[a]	R_S[b]	Mobile phase[c]
2	Fe	CH_3	OH	1.13	1.56	65/35
3	Fe	CH_3	OCH_3	1.12	1.58	70/30
4	Fe	$CH(CH_3)_2$	OH	1.08	1.00	70/30
5	Fe	C_6H_5	OH	1.00	0	60/40
6	Fe	CH_3	SC_6H_5	1.39	2.27	90/10
7	Fe	CH_3	SCH_2COOH	1.33	1.40	50/50
8	Fe	CH_3	SCH_2CH_2OH	1.23	2.13	90/10
9	Fe	$CH(CH_3)_2$	SCH_2CH_2OH	1.13	1.52	70/30
10	Fe	C_6H_5	SCH_2CH_2OH	1.06	1.15	50/50
11	Fe	D	OH	1.00	0	70/30
12	Fe	CH_3	NH_2	1.17	0.44	60/40
13	Fe	CH_3	$NHCH_2C_6H_5$	1.11	0.56	65/35
14	Fe	CH_3	$N(CH_3)_2$	1.30	0.74	80/20
15	Ru	CH_3	OH	1.11	1.56	65/35
16	Os	CH_3	OH	1.08	1.50	60/40

[a] α = selectivity factor.
[b] R_S = resolution factor.
[c] Numbers represent the volume ratio (v/v) of methanol to water in an isocratic separation. Flow rate = 1 ml/min.

separated, and the lack of enantioseparation of *rac*-deuterioferrocenylmethanol (**11**) was ascribed to the difficulty to distinguish between nonionizable hydrogen and deuterium.

Starting from the 1980s, the Co(acac)$_3$ complex (acac = acetylacetonate) (**17**) was frequently used as a test probe for testing the enantioseparation ability of polysaccharide- [13,14] and CD-based [15] chiral stationary phases (CSPs). Given this background, in this review, representative applications of LC techniques for the enantioseparation of organometallic compounds and metal complexes will be presented and discussed, describing the evolution of the field over time, starting from the high-performance liquid chromatography (HPLC) analyses developed in the 1990s, until the most recent applications for the enantioseparation of chiral metal clusters. Applications performed under supercritical fluid chromatography (SFC) conditions will be also presented. Given that the applications for the enantioseparation of planar chiral ferrocenes were recently reviewed [16], in this review only the most recent applications in this field will be described.

For clarity, in the text as well as in figures and tables included in this review, chiral compounds and classes of structurally related compounds

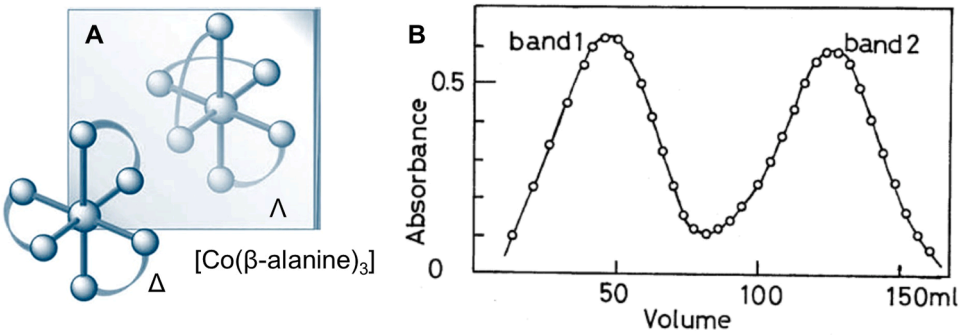

Fig. 2. (A) Δ and Λ enantiomers of chiral-at-metal complexes, adapted with permission from Ref. [5]; (B) Elution curve of [Co(β-alanine)$_3$] (elution rate: 4 ml/20 min), adapted with permission from Ref. [11]. (For interpretation of the references to color in this figure legend, the reader is referred to the web version of this article.)

Table 2
Polysaccharide-based chiral columns and corresponding chiral selector mentioned in this review.

Chiral column	Type	Chiral selector
Chiralpak AD	Coated	Amylose *tris*(3,5-dimethylphenylcarbamate)
Chiralpak AS	Coated	Amylose-*tris*((*S*)-α-methylphenylcarbamate)
Chiralpak IB	Immobilized	Cellulose *tris*(3,5-dimethylphenylcarbamate)
Chiralpak IC	Immobilized	Cellulose *tris*(3,5-dichlorophenylcarbamate)
Chiralpak IE	Immobilized	Amylose *tris*(3,5-dichlorophenylcarbamate)
Chiralpak IF	Immobilized	Amylose *tris*(3-chloro-4-methylphenylcarbamate)
Chiralpak IG	Immobilized	Amylose *tris*(3-chloro-5-methylphenylcarbamate)
Chiralcel OA	Coated	Cellulose triacetate
Chiralcel OB	Coated	Cellulose tribenzoate
Chiralcel OC	Coated	Cellulose triphenylcarbamate
Chiralcel OD	Coated	Cellulose *tris*(3,5-dimethylphenylcarbamate)
Chiralcel OF	Coated	Cellulose *tris*(4-chlorophenylcarbamate)
Chiralcel OG	Coated	Cellulose *tris*(4-methylphenylcarbamate)
Chiralcel OJ	Coated	Cellulose *tris*(4-methylbenzoate)
Chiralcel OK	Coated	Cellulose tricinnamate
Lux Amylose-1	Coated	Amylose *tris*(3,5-dimethylphenylcarbamate)
Lux Amylose-2	Coated	Amylose *tris*(5-chloro-2-methylphenylcarbamate)
Lux i-Amylose-3	Immobilized	Amylose *tris*(3-chloro-5-methylphenylcarbamate)
Lux Cellulose-1	Coated	Cellulose *tris*(3,5-dimethylphenylcarbamate)
Lux Cellulose-2	Coated	Cellulose *tris*(3-chloro-4-methylphenylcarbamate)
Lux i-Cellulose-5	Immobilized	Cellulose *tris*(3,5-dichlorophenylcarbamate)

mentioned as chiral analytes will be identified by sequential numbering.

2. Decade 1990s

Most enantioseparations developed in this decade were performed by using polysaccharide-based CSPs, whereas CSPs based on CDs and glycopeptides as well as brush-type CSPs were used to a lesser degree. For this reason, polysaccharide-based chiral columns and related chiral selectors mentioned in this review are summarized in Table 2. For clarity, the enantioseparations discussed in this section are summarized in Table 3, whereas representative chiral organometallic compounds and metal complexes enantioseparated in the 1990s are depicted in Fig. 3, which includes metallocenes (**18-23**), metal arene complexes (**24-31**), metal oxides (**32**), tetracarbonyldiphosphine complex (**33**), copper (I) catenates (**34**), ten-vertex carboranes (**35** and **36**), chiral metalloporfirines (**37** and **38**), cyclooctapyrrole metal complexes (**39** and **40**), and a salen-type Mn complex (Jacobsen's catalyst) (**41**).

In 1991, Ramsden *et al.* reported the enantioseparation of 22 chiral compounds with the chemical formula (η^5-C_5R_5)M(L)(PAr_3)(X) (metal (M)/L = Re/NO, Fe/CO) (series **18** and **19**) performed by using the Chiralcel OD column and *n*-hexane/2-propanol (2-PrOH) mixtures as mobile phases [17]. For these chiral-at-metal cyclopentadienyl complexes, the impact of R (H, Me), X (H, Me, F, Cl, Br, I, CO_2Me, OCOMe, $OCOCF_3$, OCOPh, CH_2Ph, COPh, Ph, C≡CH, C≡CPh, C≡N, etc.), and M (Re, Fe) on the enantioseparation was examined based on obtained chromatographic parameters. The following trends were observed:

1. A steric effect induced by distinctive parts of the molecules could be observed: *a)* enantiomers of halide adducts (η^5-C_5R_5)Re(NO)(PPh_3)(X) (X = F, Cl, Br, I) were separated with α and resolution (R_S) increasing following the order I < Br < Cl ≈ F; *b)* pentamethylcyclopentadienyl complexes (η^5-C_5Me_5)Re(NO)(PPh_3)(X) eluted more rapidly compared to the pentadienyl analogues, with lower α and R_S; *c)* the tri-*p*-tolylphosphine complexes (η^5-C_5H_5)Re(NO)(P(p-tol)$_3$)(X) eluted more rapidly as well, whereas α increased by replacing PPh_3 to the corresponding *p*-tolyl phosphine.
2. The impact of the electronic properties was also observed, particularly on retention factors (*k*). For instance, although its resolution was not exceptional, the (η^5-C_5H_5)Re(NO)(PPh_3)(CN) complex gave the longest retention time of all the compounds examined. Interestingly, while the enantiomers of this complex were highly differentiated by the chiral NMR shift reagent Eu(hfc)$_3$ (Europium *tris*[3-(heptafluoropropylhydroxymethylene)-(+)-camphorate]), the two analytical methods provided enantiomer ratios that were in excellent agreement.
3. Enantiomers of the iron iodide complex (η^5-C_5H_5)Fe(CO)(PPh_3)(I) were separated with lower α (1.13) compared to the enantiomers of the (η^5-C_5H_5)Re(NO)(PPh_3)(I) complex (α = 1.16). The same trend was observed for the methylated derivatives. Whereas the (η^5-C_5H_5)Re(NO)(PPh_3)(Me) enantiomers were separated (α = 1.17), (η^5-C_5H_5)Fe(CO)(PPh_3)(Me) could not be resolved.

In the same year, Yamazaki *et al.* explored the enantioseparation of planar chiral metallocenes belonging to the series **20, 21**, and metal arene complexes **24-27** [18], developing successful HPLC enantioseparations for the 1-hydroxymethyl-2-methyl, 1-acetoxymethyl-2-methyl and 1-methoxycarbonyl-2-methyl derivatives of (η^6-benzene)tricarbonylchromium, tricarbonyl(η^6-cyclopentadienyl)manganese and ferrocene, and for their 3-methyl analogues, by using the Chiralcel OD column and a *n*-hexane/2-PrOH mixture (1.3 *M* 2-PrOH in *n*-hexane) as

Table 3
Representative enantioseparations of chiral metal complexes reported in the 1990s (for numbering of compounds refer to Fig. 3).

Analyte	Metal	Compound type	Chiral column or selector[a]	Mobile phase[b]	Ref.
18, 19	Re, Fe	Metal arene complexes	Chiralcel OD	*n*-hexane/2-PrOH mixtures	[17]
20, 21	Fe	Ferrocenes	Chiralcel OD	*n*-hexane/2-PrOH (1.3 *M*)	[18]
24-27	Mn, Cr	Metal arene complexes	Chiralcel OD	*n*-hexane/2-PrOH (1.3 *M*)	[18]
28-31	Cr	Metal arene complexes	(*S,S*)-Whelk-O1	*n*-hexane/2-PrOH 80:20 or /CH_2Cl_2 70:30	[19]
23	Zr	Metallocenes	Chiralcel OD	*n*-hexane/EtOH 20:1	[21]
32	Te	Metal oxides	Chiralpak AS	*n*-hexane/2-PrOH 98:2 or 95:5	[23]
33	W	Metal tetracarbonyl complex	Chiralcel OD	*n*-hexane/2-PrOH 90:10	[24]
20	Fe	Ferrocenes	Chiralcel OD-H	*n*-hexane/2-PrOH mixtures	[25]
22	Fe	Ferrocenes	β- and γ-CD	MeOH/H_2O 50:50	[26]
22	Fe	Ferrocenes	Vancomycin	*n*-hexane/2-PrOH 97:3	[26]
34	Cu	Catenates	ADMPC	*n*-hexane/2-PrOH 50:50	[27]
37	Zn	Metalloporfirines	Chiralcel OD	*n*-hexane/2-PrOH 4:1	[28]
38	Zr, Ce	Metalloporfirines	CDMPC	*n*-hexane/EtOH mixtures	[29]
39,40	Pd, Cu	Cyclooctapyrroles	Chiralcel OD	*n*-hexane/2-PrOH/DEA	[30]
35,36	B	Ten-vertex carboranes	β- and acetyl-β-CD	MeOH/H_2O mixtures	[31]
41	Mn	Jacobsen's catalyst	hydroxypropyl β-CD	nonaqueous polar-organic mixture	[33]

[a] ADMPC, amylose *tris*(3,5-dimethylphenylcarbamate); CD, cyclodextrin; CDMPC, cellulose *tris*(3,5-dimethylphenylcarbamate).
[b] Numbers represent the volume ratio (v/v or v/v/v) of solvents (additives) in the mobile phase; DEA, diethylamine; EtOH, ethanol; MeOH, methanol; 2-PrOH, 2-propanol.

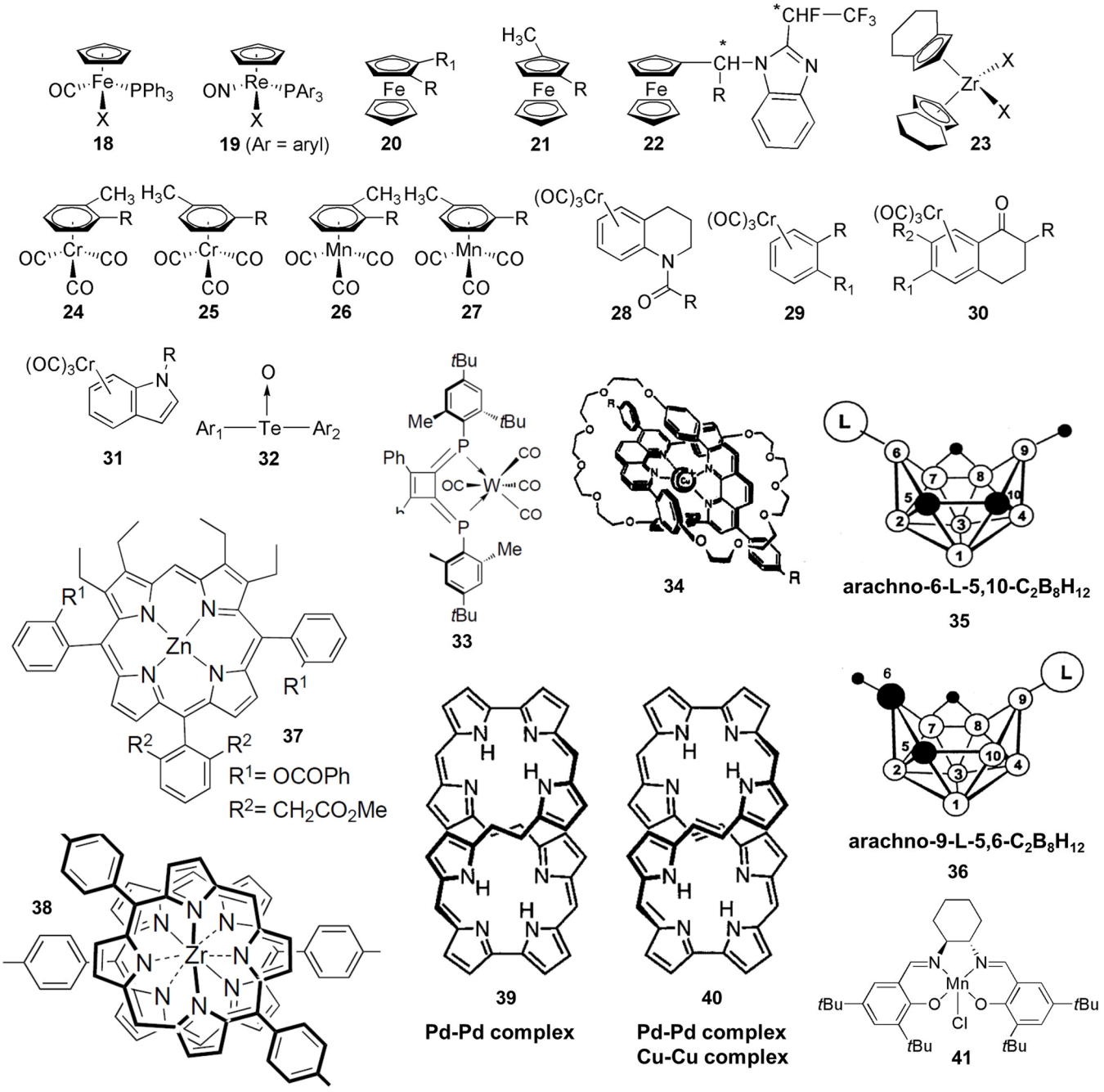

Fig. 3. Representative chiral metal complexes enantioseparated by liquid chromatography in the 1990s. Structures of compounds **33**-**41** adapted with permission from Refs. [24,27,28,30,31].

mobile phase. The polysaccharide-based Chiralcel OA, OB, OK, OC chiral columns, and the polymethacrylate-based Chiralpak OT(+) and OP(+) chiral columns exhibited limited performances for the separation of these series of complexes.

Later, Pirkle and Villani examined the HPLC enantioseparation of thirty-four disubstituted tricarbonyl (η^6-arene)-chromium complexes, belonging to the series **28**-**31** and having planar chirality, by using the (*S,S*)-Whelk-O1 chiral column and *n*-hexane/2-PrOH 80:20 v/v as mobile phase while, in some cases, *n*-hexane/CH_2Cl_2 70:30 v/v [19]. The (*S,S*)-Whelk-O1 is based on a brush-type CSP featuring active sites comprised of clefts formed by the perpendicular disposition of the π-acidic 3,5-dinitrobenzamide group relative to the π-basic naphthyl group. Thirty of the thirty-four compounds were enantioseparated with α values ranging from 1.04 to 2.74. A mechanistic hypothesis accounting for the enantiodifferentiation was proposed. The authors hypothesized that the arene moiety, using the face *anti* to the tricarbonylchromium, enters the cleft and undergoes simultaneous face-to-face and face-to-edge π-π interactions with the aromatic moieties of the cleft (the π-acidic 3,5-dinitrobenzamide group and the π-basic naphthyl group). Hydrogen bonding formation could provide a third attractive interaction, contributing to the enantiodifferentiation mechanism. This mechanism was shown to be consistent with results based on NMR spectroscopy.

Following the previous successful analytical resolution of racemic ethylenebis(4,5,6,7-tetrahydro-1-indenyl)zirconium derivatives **23** by HPLC on Chiralcel OD [20], in 1997 Okamoto's group reported the HPLC preparative separation of 13 mg of *rac*-ethylenebis(4,5,6,7-tetrahydro-1-indenyl)zirconium-2,2'-biphenolate complex (**23**, X,X =

OC_6H_4-C_6H_4O-) to obtain the complex in enantiopure form for further applications in asymmetric catalysis [21]. The preparative separation was performed with the Chiralcel OD column (50 × 2 cm) by using *n*-hexane/EtOH 20:1 v/v as mobile phase (flow rate = 10 ml/min).

In 1997, following the results obtained by Shimizu and Kobayashi for the medium pressure enantioseparation of chiral selenoxides using a column packed with (*R*)-*N*-(3,5-dinitrobenzoyl)phenylglycine/aminopropylsilica and *n*-hexane/2-PrOH mixtures as mobile phases [22], Shimizu *et al.* studied the separation of the enantiomers of chiral telluroxides belonging to the series **32** by using Chiralpak AS (10 × 250 mm) as chiral column and *n*-hexane/2-PrOH mixtures as mobile phases [23]. The authors examined four different telluroxides with different combinations of Ar_1/Ar_2 substituents. The analytical HPLC enantioseparation of the telluroxide with Ar_1 = mesityl and Ar_2 = 2,4,6-triisopropylphenyl was examined with Chiralpak AS and AD, and Chiralcel OB, OJ, OC, OD, OF, and OG as chiral columns, obtaining the best enantioseparation with Chiralpak AS. However, on-column racemization was observed for this compound (Fig. 4A). Using the AS column, telluroxides with Ar_1 = mesityl and Ar_2 = 2,4,6-tri-*t*-butylphenyl (Fig. 4B) and with Ar_1 = phenyl and Ar_2 = 2,4,6-tri-*t*-butylphenyl (Fig. 4C) were also enantioseparated, while telluroxide with Ar_1 = phenyl and Ar_2 = 2,4,6-triisopropylphenyl, featuring less bulky substituents, remained unresolved. These results showed that a substituent bulkier than the 2,4,6-triisopropylphenyl group was needed to inhibit racemization. On the other hand, with the bulkier 2,4,6-tri-*t*-butylphenyl, changing phenyl, as Ar_1 group, to mesityl was detrimental to enantioselectivity.

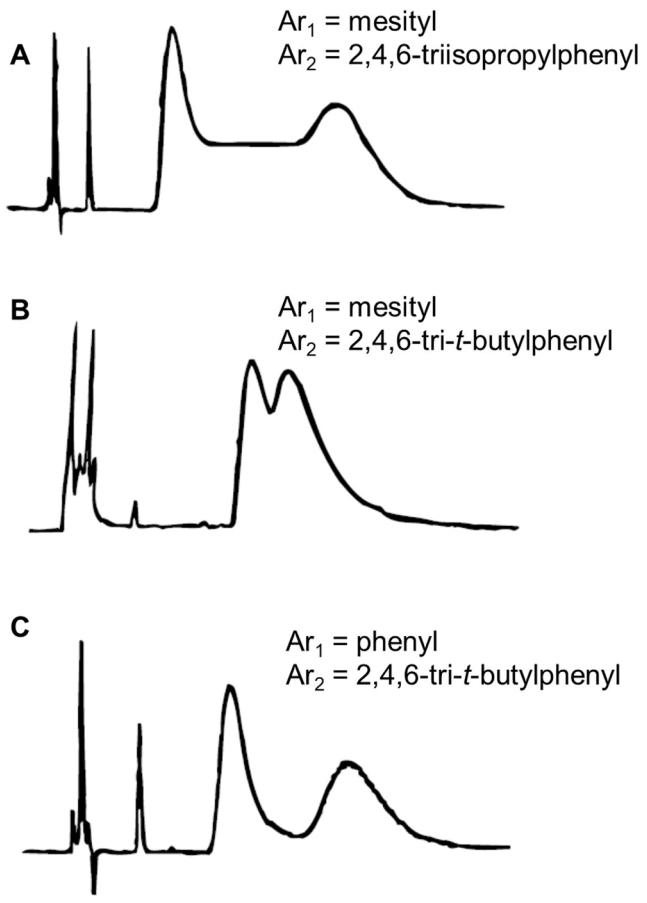

Fig. 4. Enantioseparation of chiral telluroxides $Ar_1(Ar_2)Te{\rightarrow}O$ (**32**) with Chiralpak AS and *n*-hexane/2-PrOH mixtures as mobile phases: (A) Ar_1 = mesityl, Ar_2 = 2,4,6-triisopropylphenyl, (B) Ar_1 = mesityl, Ar_2 = 2,4,6-tri-*t*-butylphenyl, (C) Ar_1 = phenyl, Ar_2 = 2,4,6-tri-*t*-butylphenyl. Adapted with permission from Ref. [23].

In the same year, Yoshifuji *et al.* developed the enantioseparation of the W tetracarbonyl complex of 3,4-diphosphinidenecyclobutene protected with the 2,4-di-*t*-butyl-6-methylphenyl group (**33**) obtained as *anti*-rotational isomer along with the *syn*-isomer [24]. The enantiomers of the *anti*-isomer were separated by using Chiralcel OD as chiral column and *n*-hexane/2-PrOH 90:10 v/v as mobile phase.

In the late 1990s, pure enantiomers of planar chiral ferrocenes of general structure **20** were prepared by asymmetric synthesis and analysed by enantioselective HPLC for the determination of the enantiomeric excess. For this purpose, Riant *et al.* used Chiralcel OD-H as chiral column and *n*-hexane/2-PrOH mixtures as mobile phases [25]. In other cases, chiral ferrocenes were prepared in racemic form, and enantiomers of high purity were obtained by chromatographic separation. Snegur *et al.* separated the enantiomers of chiral ferrocenes belonging to the series **22** by using different chiral columns based on β- and γ-CDs (mobile phase = MeOH/H_2O 50:50 v/v), and vancomycin (mobile phase = *n*-hexane/2-PrOH 97:3 v/v) [26].

In this same decade, the enantioseparations of some large-sized chiral compounds were also developed. The enantiomers of the chiral copper (I) catenates $[1Cu]^+$ and $[2Cu]^+$ (**34**) were separated by using a column based on amylose *tris*(3,5-dimethylphenylcarbamate) (ADMPC) as chiral selector and *n*-hexane/2-PrOH 50:50 v/v as mobile phase [27], although baseline resolution was not obtained in these cases. Polysaccharide based columns were also used with *n*-hexane-based mobile phases for the enantioseparation of chiral metalloporphyrines **37** (M = Zn) [28] and **38** (M = Zr) [29]. It is worth mentioning that the metalloporphyrin containing Ce as metal centre was also enantioseparated under similar conditions [29].

In 1999, Werner *et al.* studied the enantioseparation of cyclooctapyrrole metal complexes **39** and **40** [30] by using cellulose-based chiral columns with *n*-hexane/2-PrOH (0.25 %)/diethylamine (0.1-0.2 %) mixtures as mobile phases (Table 4). Chiralcel OD was used as analytical column, while the enantioseparation at preparative scale required the preparation of an appropriate column. For this purpose, spherical silica gel with a pore size of 120 Å and a particle size of 3 μm (Hyperprep) was used. After successive treatment with dimethyloctylchlorosilane and trimethylchlorosilane, the obtained octyl-silica gel was coated with 10 wt % of cellulose *tris*(3,5-dimethylphenylcarbamate) (CDMPC). The CSP (CDMPC-C_8) was packed in a thermostated glass column (25 × 300 mm) and used by cyclic medium pressure chromatography (closed loop technique). Whereas these metal complexes could be well separated on the preparative phase CDMPC-C_8, baseline enantioseparation by using Chiralcel OD as chiral column under analytical conditions could be obtained only for Pd-Pd complex **40**.

Native and acetyl β-CDs were used with MeOH/H_2O mixtures as mobile phases for the enantioseparation of two ten-vertex carborane series, i.e. the *exo*-6-L-arachno-5,10-$C_2B_8H_{12}$ (L = secondary or tertiary amino group) **35** and the *exo*-9-L-arachno-5,6-$C_2B_8H_{12}$ (L = NH_3, primary or secondary amino group) **36** [31]. Deep differences in enantioselectivities were observed for native and acetyl β-CD-based CSPs. The acetyl β-CD-based chiral column proved to be more suitable for the enantioseparation of chiral cage carbaborane and metalloborane species, especially those bearing groups with hydrogen bond donor properties.

The studies discussed in this section so far are based on the comparative analysis of closely related chiral analytes on one or more chiral columns to explore the enantioseparability of certain classes of compounds and/or to evaluate the performances of selected chiral columns towards specific types of chiral compounds. On the other hand, several applications reported in 1990s highlighted the importance of using enantioselective LC for determination of the enantiomeric purity of chiral catalysts. This is a very critical issue in asymmetric synthesis, in particular when a chiral catalyst or auxiliary is used to generate an additional stereogenic centre in a chiral substrate. In this case, the level of stereoisomeric impurity in the final product can be greater or less than that present in the chiral reagent because of kinetic effects [32]. Thus,

Table 4
Chromatographic data of the analytical and preparative enantiomeric separation of the cyclooctapyrrole metal complexes **39** and **40** [30]: *n*-hexane + 2-PrOH (0.25 %) and DEA (0.1-0.2 %); room temperature; R_S, resolution.[a]

		Analytical: HPLC, Chiralcel OD				Preparative: Medium pressure LC (CDMPC-C_8)			
Analyte	Metal	k_1	k_2	α	R_S	k_1	k_2	α	R_S
39	Pd-Pd	0.25	0.32	1.28	0.96	0.19	1.2	6.3	4.9
40	Pd-Pd	0.55	1.05	1.91	3.43	1.15	8.51	56.7	27
40	Cu-Cu	0.36	9.36	1	0	0.15	1.53	10	8.1

[a] 2-PrOH, 2-propanol; DEA, diethylamine.

determination of the enantiomeric purity is highly important, also using methods that enable determination of values as little as 0.01 % of one enantiomer in the presence of 99.99 % of the other. In 1998, Zukowski reported a HPLC method for the chiral analysis of the commercially available Jacobsen's catalyst (**41**) by using a hydroxypropyl β-CD CSP with a nonaqueous polar-organic mobile phase [33]. The method was applied to the Jacobsen's catalyst quality control process, providing synthetic chemists with a tool for enantiomeric purity determination when larger amounts of the catalyst are purchased as produced. Seminal studies for quality control of chiral (metal) catalysts and auxiliaries were performed by the group of Armstrong in the 1990s [32] and in the 2010s [34,35]. For this purpose, chiral columns based on native and derivatized CDs, macrocyclic glycopeptides, and cyclofructans were used with different types of mobile phases.

The applications described in this section, show that, in the 1990s, the combination Chiralcel OD/*n*-hexane-based mobile phases was used in most cases for the enantioseparation of metal-containing chiral compounds, and several chiral catalysts prepared in this decade as racemates were successfully enantioseparated for applications in asymmetric synthesis using the combination polysaccharide-based chiral columns and *n*-hexane-based mobile phases. For instance, in the second half of the 1990s, the first semipreparative HPLC enantioseparations of planar chiral ferrocenes were successfully performed by Fu's group by using, in most cases, Chiralcel OD as a chiral column under normal phase elution mode [36,37]. On the other hand, it is worth mentioning that in 1990s other polysaccharide-based chiral columns which will be widely used in the subsequent decades were either not commercialized yet or not as popular as Chiralcel OD at that time.

3. Decade 2000s

If the 1990s were dominated by using the normal phase elution mode for the HPLC separation of the enantiomers of chiral organometallic compounds and metal complexes, in the 2000s polar organic solvents and aqueous organic conditions were also frequently used for this purpose. The enantioseparations discussed in this section are summarized in Table 5.

In 2000, Gasparrini *et al.* reported the enantioseparation of a series of chiral tris-diimine ruthenium(II) complexes by HPLC on a CSP prepared by covalent attachment of the glycopeptide antibiotic teicoplanin to isocyanate activated silica gel [38]. The enantiomers of $[Ru(L)_3]^{2+}$ (**42-44**) [L = 2,2'-bypyridine (bpy), 1,10-phenanthroline (phen) and 4, 7-diphenyl-1,10-phenanthroline (dpphen)] were enantioseparated with a preference for the Δ isomer (Fig. 5) by using acetonitrile (ACN)/-MeOH/ammonium acetate ($AcONH_4$) 0.1 M 60:20:20 v/v/v mobile phase. For the mixed-ligand complexes $[Ru(bpy)_2pztr]^+$ **45** and **46**, and $[Ru(bpy)_2pytr]^+$ **47** and **48** (Hpztr = 3-(pyrazin-2-yl)-1,2,4-triazole, Hpytr = 3-(pyridin-2-yl)-1,2,4-triazole) (Fig. 6), where the triazole unit is bound to the metal centre either through the N^2 or the N^4 nitrogen of the ring, the teicoplanin-based CSP resolved both enantiomers and regioisomers. Diastereo- and enantioselective association was also observed between the used CSP and the stereoisomers of the dinuclear complex $[Ru(bpy)_2)_2bpt]^{3+}$ (Hbpt = 3,5-bis(pyridin-2-yl)-1,2,4-triazole) **49** (Fig. 7A). For these species, one of the two metals was N^2-bound to the centrale triazole unit, whereas the other was N^4-bound.

Table 5
Representative enantioseparations of chiral metal complexes reported in the 2000s (M = metal).

M	Compound type[a]	Chiral column or selector[b]	Mobile phase[c]	Ref.
Ru	Tri-diimine complexes	Teicoplanin	ACN/MeOH/ $AcONH_4$ 0.1M 60:20:20	[38]
Ru	Dinuclear polypyridyl complexes	CD-based CSPs	Reversed-phase mobile phases	[39]
Ru	Polypyridyl complexes	Glycopeptides	Reversed-phase mobile phases	[40]
Fe	Ferrocenes	Chiracel OD-H	*n*-hexane/2-PrOH 90:10	[41]
Fe	Ferrocenes	Chiralcel OD, OD-H, γ-CD	*n*-hexane/2-PrOH mixtures	[42]
Fe	Ferrocene	Chiralcel OD and OJ	*n*-hexane/2-PrOH mixtures	[43]
Fe	Ferrocene	Home-made β-CD	ACN/MeOH/AA/ TEA 99:1:0.1:0.1	[44]
Fe	Ferrocene	Home-made β-CD	ACN/H_2O mixtures	[46]
Fe	Ferrocene	Home-made β-CD	ACN/H_2O mixtures	[47]
M[d]	Tetrahendane-type clusters	ADMPC	*n*-hexane/2-PrOH mixtures	[48]
Zn	Dinuclear bis (dipyrromethene) complexes	Chiralcel OD	MeOH 100 %	[49]
M[e]	Extended metal atom chain complexes	Vancomycin-based CSP	ACN/MeOH-based mixtures	[50]
Ir	heteroleptic (C^N)$_2$Ir(III) (acac)	Chiralpak AD-H	30 % or 40 % MeOH or EtOH in CO_2	[52]

[a] acac, acetylacetonate.
[b] ADMPC, amylose *tris*(3,5-dimethylphenylcarbamate); CD, cyclodextrin.
[c] Numbers represent the volume ratio (v/v or v/v/v) of solvents (additives) in the mobile phase; AA, acetic acid; ACN, acetonitrile; $AcONH_4$, ammonium acetate; EtOH, ethanol; MeOH, methanol; 2-PrOH, 2-propanol; TEA, triethylamine.
[d] M = Co, Cr, Fe, Mo, Ru, Se.
[e] M = Co, Cu, Ni.

Consequently, compound **49** exists as a couple of diastereomers, i.e. homochiral ΔΔ and ΛΛ and heterochiral ΛΔ and ΔΛ. As a result, four peaks were observed in the HPLC chromatogram (Fig. 7B) which were assigned to the homo- (first and fourth eluted) and heterochiral (second and third) diastereomers.

Later, dinuclear chiral Ru(II) complexes were enantioseparated by Armstrong's group by using CD-based [39] and macrocyclic glycopeptide CSPs [40] under reversed-phase mode.

As in the previous decade, several enantioseparations of chiral ferrocenes were reported under normal phase conditions by using polysaccharide-based (CSPs) [41–43] and, in some cases, CD-based CSPs [42]. On the other hand, enantioseparations of chiral ferrocenes by using polar organic solvents and aqueous organic mixtures as mobile phases were also reported. In 2002, Mayr *et al.* [44] reported the first analytical study on the enantioseparation of ferrocenes containing the carbonyl moiety as distinctive group, showing that the carbonyl moiety

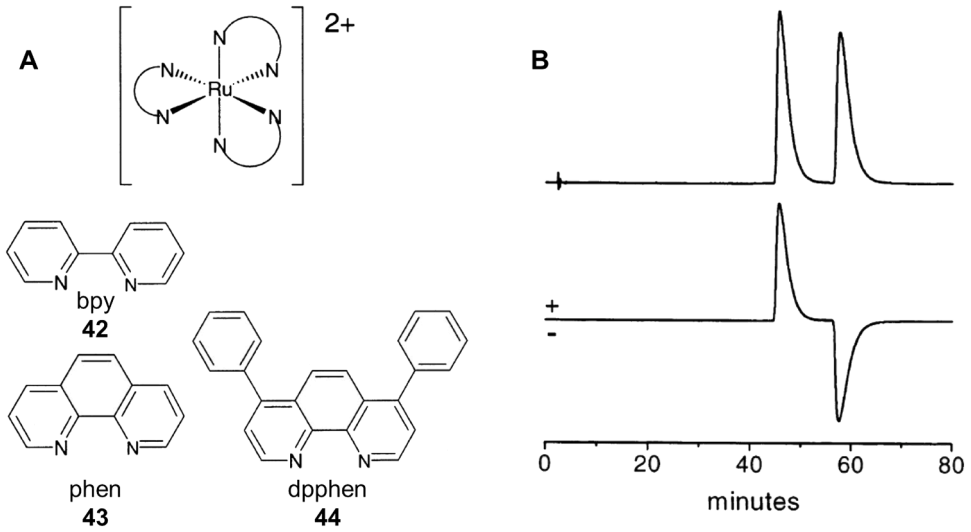

Fig. 5. (A) Structure of homoleptic polypyridyl complexes **42**-**44** (N–N = bpy, phen or dpphen, respectively); (B) enantioselective chromatography of $[Ru(phen)_3]^{2+}$ **43** on a teicoplanin-based CSP and relative circular dichroism (CD) trace. Adapted with permission from Ref. [38].

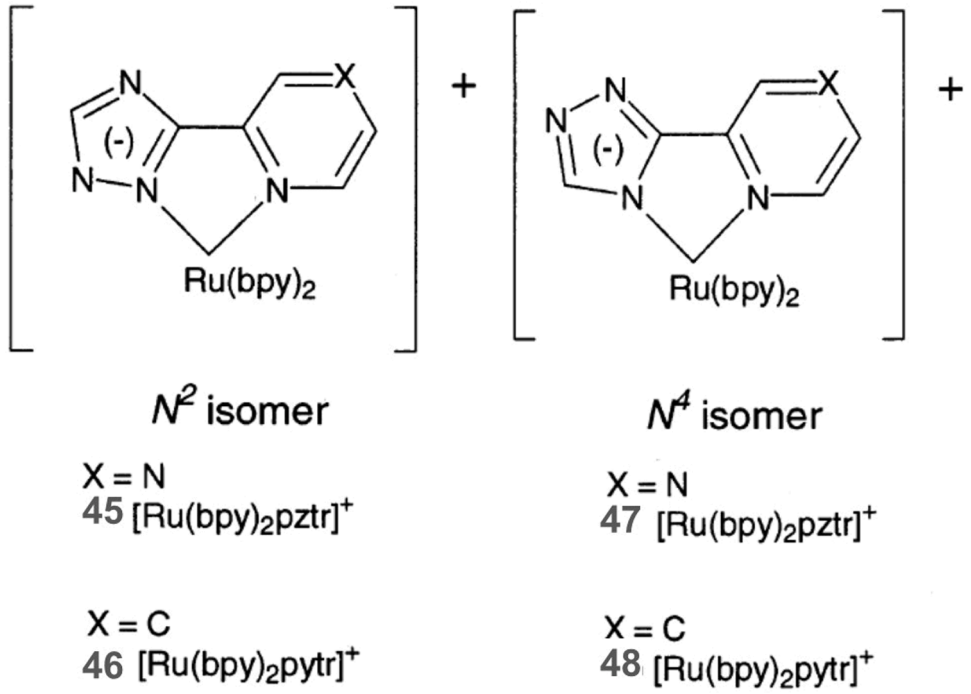

Fig. 6. Structure of coordination isomers of pyrazine triazole-containing $Ru(bpy)_2$ complexes (X = N, **45** and **47**; X = C, **46** and **48**). Adapted with permission from Ref. [38].

proved to be essential for achieving successful enantioseparation. Indeed, the enantioseparation of planar chiral ferroceno[2,3-a] inden-1-ones (**50**) and derivatives (Fig. 8) was explored by using five homemade β-CD-based chiral columns under polar organic conditions (ACN/MeOH/acetic acid (AA)/triethylamine (TEA) 99:1:0.1:0.1 v/v/v/v, T = 0 °C). Whereas ferroceno[2,3-a]inden-1-one (**50**) and derivatives could be enantioseparated with $1.62 \leq \alpha \leq 2.15$, ferroceno[2, 3-a]indene (**51**) and the alkoxyferroceno[2,3-a]indene (**52**) were not resolved under the explored conditions. These observations revealed that the enantioseparation of nonpolar chiral planar ferrocenes may be rather challenging, this fact representing a still open issue tackled only recently [16,45]. Chen *et al.* used ACN/H_2O mixtures to enantioseparate chiral ferrocenes with a series of home-made CSPs based on β-CD derivatives [46,47].

In this decade, advancement in molecular design favoured the development of new motifs in organometallic chemistry and, consequently, the development of enantioseparation methods for fast determination of the enantiomeric purity of products of asymmetric synthesis, or for semipreparative recovery of pure or enriched enantiomers, was required. This tendency will be more evident in the next decades 2010s and 2020s with the development of multinuclear metal clusters. Wang *et al.* reported the enantioseparation of the series of chiral heterometal tetrahedral clusters **53**-**57** (Fig. 9A) under normal phase by using an ADMPC-based CSP prepared by coating the selector on small-particle aminopropylated silica gel [48]. The results showed that the structure and the concentration of the alcohol modifier in the mobile

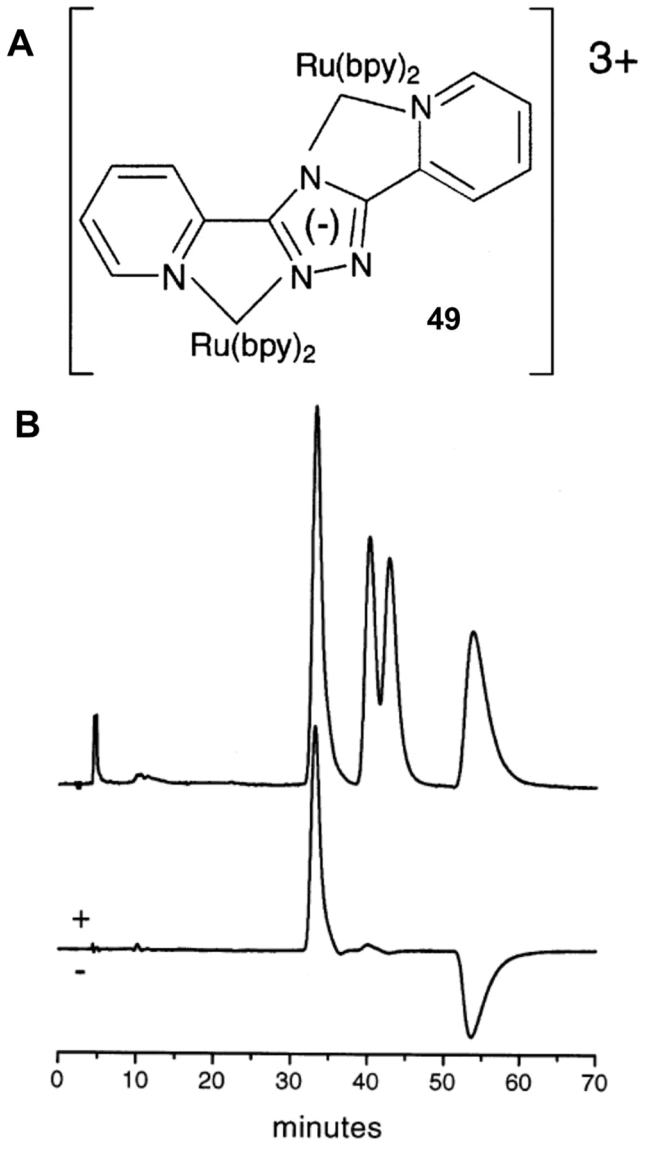

Fig. 7. (A) Structure of dinuclear complex **49**; (B) Enantio- and diastereoselective chromatography of $[Ru(bpy)_2)_2bpt]^{3+}$ (Hbpt = 3,5-bis(pyridin-2-yl)-1,2,4-triazole) **49** on a teicoplanin-based CSP and related circular dichroism trace. Adapted with permission from Ref. [38].

phase had a large effect on the enantioseparation. Furthermore, both the metal, in the tetrahedral core, and the ligand coordinated to the atom in the tetrahedral core had significant effects on the enantioseparation of the chiral clusters (Fig. 9B). Later, by using polar organic elution mode, Wood *et al.* reported the enantioseparation of stereochemically stable double-helicate dinuclear (Zn-Zn) complexes of bis(dipyrromethene)s with Chiralcel OD in pure MeOH as mobile phase [49]. Armstrong's group studied the enantioseparation of the complexes **58**-**62** (Table 6) consisting of extended metal atom chains containing a linear metal chain surrounded by various ligands. Most complexes were of the form $M_3(dpa)_4X_2$ (**58**-**60**), where M = metal, dpa = 2,2'-dipyridylamide, and X = various anions [50]. The ligands formed helical coils about the metal chain, which resulted in the chiral complexes. The complexes containing the metals Co (**59**) and Cu (**58**) were partially separated in polar organic mode (ACN/MeOH-based mixtures) using a vancomycin-based CSP. Under similar conditions, complexes **60** and **61** with Ni as metal and varying anions could be baseline separated. In this case, the polar organic mode was used because of the instability of these compounds in aqueous mobile phases. Furthermore, polar organic

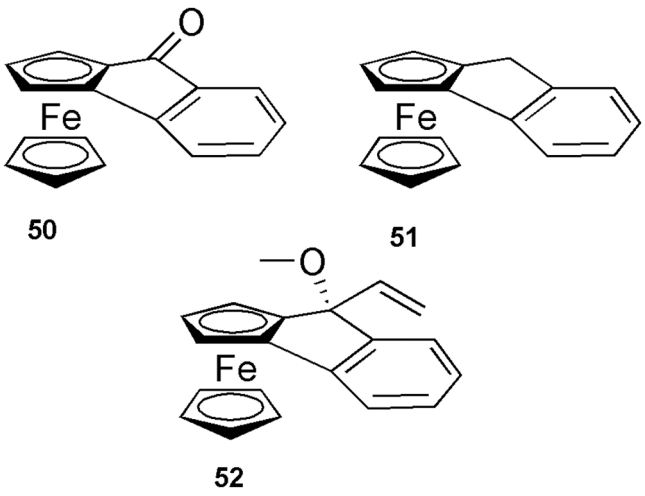

Fig. 8. Structures of chiral ferrocenes **50**-**52**.

solvents were suitable for preparative separations. Only complex **62** (M = Ni) was separated under normal phase conditions. For Ni-containing complexes, the chirality was determined using vibrational circular dichroism, electronic circular dichroism, optical rotatory dispersion, and density functional theory calculations [51]. Polarimetric measurements on the resolved enantiomers of $Ni_3(dpa)_4Cl_2$ (**61**) indicated that they had extraordinarily high specific rotations (on the order of 5000 deg cc/g dm) [50].

Enantiomers of heteroleptic $(C^N)_2Ir(III)(acac)$ (where C^N = a substituted 2-phenylpyridine and acac = acetylacetonate) luminophores (**63**) were separated in preparative scale by Coughlin *et al.* with Chiralpak AD-H in SFC (40 % MeOH or EtOH in CO_2 at a back pressure of 100 bar with a flow rate of 50 mL/min and temperature of 35 °C) recovering multimilligram amounts of enantiomers with high enantiomeric purity (*ee* > 99 %) [52].

4. Decade 2010s

In this decade, several metal clusters based on Au as metal core were enantioseparated by using Lux Cellulose-1 and *n*-hexane-based mixtures as mobile phases. In these clusters, although the bulk phase of metals is symmetric, their surfaces can become chiral by adsorption of specific molecules. Even achiral molecules can induce topologically chiral surfaces [53]. The interest in the enantioseparation of these nanomaterials is related to the evidence that chiral nanocrystals may interact enantioselectively with biomolecules and biological tissue [54]. These enantioseparations along with others developed in this decade are summarized in Table 7.

In 2012, Dolamic *et al.* reported the first separation of the enantiomers of a gold cluster protected by achiral thiolate groups, $Au_{38}(SCH_2CH_2Ph)_{24}$ (**64**), achieved by enantioselective HPLC with Lux Cellulose-1 (*n*-hexane/2-PrOH 80:20 v/v, 2 ml/min, t_1 = 8.45 min, t_2 = 17.45 min) [53]. The chirality of the nanocluster arises from the chiral arrangement of the thiolate groups on its surface, forming 'staple motifs'. In the same year, Knoppe *et al.* reported the enantioseparation of the $Au_{40}(SCH_2CH_2Ph)_{24}$ (**65**) (Fig. 10A) (Lux Cellulose-1, *n*-hexane/2-PrOH 90:10 v/v, 1 ml/min) [55], but baseline enantioseparation was not obtained in this case. In 2013, Zeng *et al.* reported the crystal structure of a nanocluster formulated as $Au_{28}(TBBT)_{20}$ (TBBT = 4-tert--butylbenzenethiolate) (**66**) (Fig. 10B). This nanocluster exhibits a rod-like Au_{20} kernel consisting of two interpenetrating cuboctahedra [56]. The kernel is protected by four dimeric "staples" (-SR-Au-S-R-Au-SR-) and eight bridging thiolates (-SR-). The unit cell of **66** single crystals was shown to contain a pair of enantiomers. In this system, the origin of chirality was found in the rotating arrangement of the four

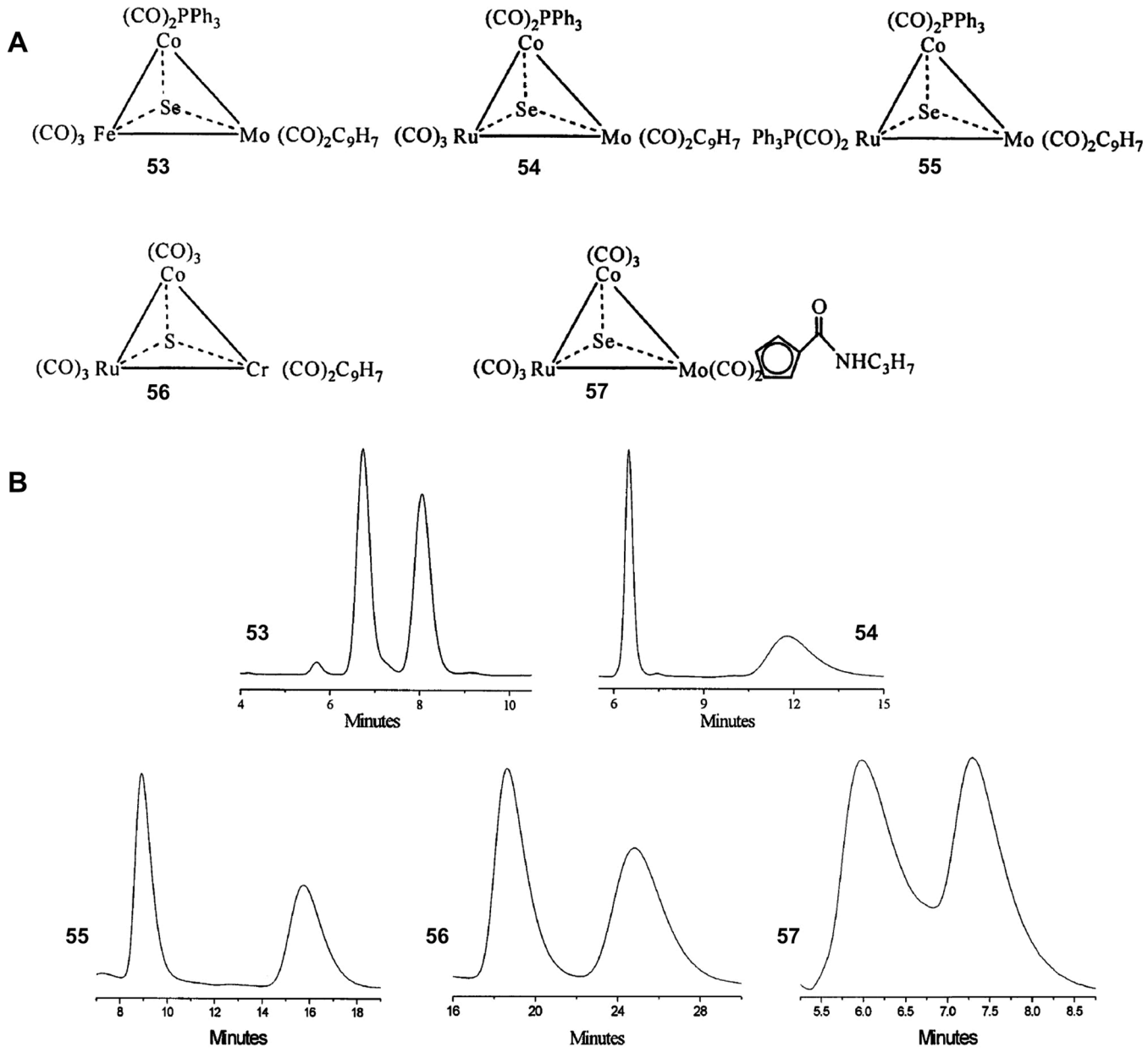

Fig. 9. (A) Structures of chiral tetrahedrane-type clusters **53**-**57**; (B) Chromatograms of enantioseparation of the clusters **53**-**57** with an ADMPC-based CSP: mobile phase, *n*-hexane/1-PrOH 90:10 v/v for **53**, *n*-hexane/EtOH 90:10 v/v for **54**, *n*-hexane/1-butanol 90:10 v/v for **55**, *n*-hexane/2-PrOH 90:10 v/v for **56** and **57**. Adapted with permission from Ref. [48].

dimeric staples as well as the arrangement of the bridging thiolate groups (quasi-D_2 symmetry). The enantiomers were separated by chiral HPLC (Lux Cellulose-1, *n*-hexane/2-PrOH 80:20 v/v, 0.3 ml/min, 10 °C) and characterized by circular dichroism spectroscopy. Also in this case, baseline enantioseparation was not obtained under the adopted conditions.

In 2013, Lin *et al.* developed the first enantioseparation of a chiral-at-metal osmabenzene complex, the {Os(II)[CHC(PPh_3)CHC(PPh_3)CH]($C_9H_6NO)_2$}Cl (**67**) (Fig. 11), by using a CSP synthesized by immobilizing heptakis(6-azido-6-deoxy-2,3-di-*O*-*p*-chlorophenylcarbamoylated)-β-CD onto silica gel [57]. The enantioseparation was studied by using various elution modes, and the best result was obtained by using EtOH as mobile phase with NH_4NO_3 (0.05 mol L^{-1}) (pH 4.27).

In 2015, the enantiomeric separation of 21 ruthenium (II) polypyridyl complexes (**68**-**88**) was investigated by Armstrong's group by using cyclofructan-based CSPs in the polar organic mode (Table 8) [58]. Aromatic derivatives on the chiral selectors proved to be essential for enantioselectivity. The *R*-napthylethyl carbamate functionalized cyclofructan 6 (LARIHC CF6-RN), as chiral column, proved to be the most effective overall, while the dimethylphenyl carbamate cyclofructan 7 (LARIHC CF7-DMP) showed complementary selectivity. The combination of acid and base additives was necessary for optimal separations. In terms of mechanism, the retention factor vs. acetonitrile/methanol ratio plot showed a U-shaped retention curve, indicating that different interactions took place at different polar organic solvent compositions. The separation results indicated that π–π interactions, steric effects, and hydrogen bonding contributed to the enantiomeric separation of ruthenium (II) polypyridyl complexes with cyclofructan CSPs in the polar organic mode.

In this decade, the use of immobilized polysaccharide-based chiral columns allowed the enantioseparation of new metal complexes designed and prepared as new catalysts, also using mobile phases containing nonstandard solvents. In this frame, a series of helicene metallocenes (**89**) (Chiralpak IF, *n*-hexane/dichloromehane 3:1) [59],

Table 6
Retention factor (k), selectivity (α), and resolution (R_S) for the enantioseparation of metal complexes **58**-**62** with a vancomycin-based CSP along with optimized separation conditions.

N.	Formula[a]	k	α	R_S	Separation condition[b]
58	$Cu_3(dpa)_4Cl_2$	2.02	1.35	1.35	ACN/MeOH 80:20 v/v + 0.3 % NH_4TFA at 1 ml/min
59	$Co_3(dpa)_4Cl_2$	2.44	1.08	1.10	ACN/MeOH 90:10 v/v + 0.3 % NH_4NO_3 at 0.4 ml/min
60	$Ni_3(dpa)_4Cl_2$	2.06	1.20	1.55	ACN/MeOH 90:10 v/v + 0.4 % NH_4NO_3 and 0.2 % NH_4TFA, 0.4 ml/min
61	$Ni_3(dpa)_4(NCCH_3)_2(PF_6)_2$	3.50	1.20	1.50	ACN/MeOH 97:3 v/v + 0.15 % NH_4TFA at 0.4 ml/min
62	$Ni_3(epapda)_4(Ph_4B)_2$	10.10	1.06	1.35	Heptane/1-PrOH 97:3 at 1.0 ml/min

[a] dpa = 2,2'-dipyridylamide; epapda = N,N'-bis(4-ethylpyridyl amido pyridyl)-2,6-diaminopyridine.
[b] ACN, acetontrile; MeOH, methanol; NH_4TFA, ammonium trifluoroacetate; 1-PrOH, 1-propanol.

octahedral Rh (**90**) and Ir (**91**) complexes with tripodal tridentate ligands (Chirapak IB, ACN/H_2O 65:35, 0.1 % AA) [60], and a chiral-at-metal Ir complex (**92**) (Chiralpak IB, ACN/H_2O 50:50, 0.1 % TFA) [61] were successfully resolved.

In 2019, the first *fac*-Ir(ppy)$_3$ (ppy = 2-phenylpyridine) cage complex (**93**) was synthesized and resolved [62]. Complex **93** formed two stable (*M*) and (*P*) helical isomers which could be enantioseparated by the (*R*)-naphthylethyl derivatized cyclofructan-6 (CF6-RN) and 3, 5-dimethylphenyl derivatized cyclofructan-7 (CF7-DMP) CSPs with 100 % methanol as the mobile phase. By changing CF6-RN to CF7-DMP a reversal of enantiomer elution order could be observed (Fig. 12).

5. Decade 2020s

In this decade, advancements in experimental and computational analysis allowed to develop more efficient strategies for molecular design favouring the development of new chiral metal complexes for application in several fields. Enantioseparations discussed in this section are summarized in Table 9.

In 2021, Gaire *et al.* developed an organometallic complex that mimics an amino acid, also known as an amino acid isostere, composed of a functionalized bipyridine ligand and a *fac*-$[Re(CO)_3]^+$ centre (Fig. 13) [63]. The reaction of an achiral ligand and metal resulted in a racemic mixture of the chiral-at-metal complex **94**. This metal complex had amine and carboxy termini, a side chain type unit that can be varied, as well as the chiral metal that is analogous to the C_α of an amino acid. The racemic mixtures could be separated into enantiomers by HPLC with the Chiralcel IE as chiral column in *n*-hexane/EtOH/TFA/DEA 60:40:0.1:0.1 v/v/v/v, and the metal complex could be incorporated into peptides by using solid-phase peptide synthesis.

In the same year, Horáček *et al.* studied the first chiral HPLC separations of anionic and zwitterionic metal bis(dicarbollide) **95** and dicarba-*nido*-undecarborane **96** (Fig. 14) by using native and brominated β-CD-based CSPs and MeOH/EDTA (ethylenediaminotetraacetic acid) and MeOH/ACN/EDTA mixtures as mobile phases [64]. Boron cluster compounds are of interest due to their possible use in medicinal chemistry, mainly in the boron neutron capture anticancer therapy and as new innovative pharmacophores [65]. Later, following previous studies performed by Mangelings *et al.* for the enantioseparations of zwitterionic and anionic bis(dicarbollide) and 7,8-dicarba-*nido*-undecarborane derivatives in polar organic and normal phase LC [66], Kučera's group studied these classes of compounds on polysaccharide-based CSPs, i.e. the Lux Cellulose 1, Lux i-Cellulose 5, and Lux Amylose 1 [67]. The authors found that RPLC is a universal elution mode for the enantioseparations of zwitterionic and anionic cobalt bis(dicarbollides) on the examined polysaccharide-based columns. Different chromatographic behaviour was observed for anionic analytes on cellulose- and amylose-based CSPs in water-organic solvent mobile phases, and the concentration of additives and temperature were identified as the key parameters for the fine tuning of the separation. In 2023, the same authors explored the ability of commercially available superficially porous particle columns to enantioseparate *nido*-7, 8-$C_2B_9H_{12}$(1-) derivatives (**96**) and one neutral mixed sandwich 4-CH_3S-3-C_5H_5-Co-(1,2-$C_2B_9H_{10}$) (**97**) [68]. The most versatile column was found to be the hydroxypropylated β-CD (CDShell-RSP) that readily separated neutral **97**, zwitterionic and anionic derivatives **96** by using the polar organic elution mode.

In the same year, Pecorari *et al.* synthesized bis-aryl carbazole borane derivatives having emissive properties and axial chirality. The resolution of the thermally stable atropisomeric compound **98**, due to a B−C chiral axis, was achieved by enantioselective HPLC by using Chiralpak AD-H as chiral column with *n*-hexane/2-PrOH 97:3 v/v as mobile phase (Fig. 15) [69].

In the past two years, interesting results were reported in terms of chemistry and LC methods for the enantioseparation of chiral ferrocenes (Fig. 16). In 2022, the first analytical study on the enantioseparation of planar chiral ferrocenes under SFC conditions was reported by Lipka's group [70]. The authors analysed 1,2- and 1,3-disubstituted chiral metallocenes (M = Fe, Ru) featuring the motifs **99**-**102** by using eleven polysaccharide-based CSPs (Lux Cellulose-2, Amylose-2 and i-Amylose-3, Chiralcel OD-H and OJ-H, Chiralpak IB, IC, AD-H, AS-H, IA and IG) with carbon dioxide containing 30 % of MeOH or 2-PrOH as co-solvent. In 2023, the groups of Peluso and Mamane reported the enantioseparation of 3,3'-dibromo-5,5'-bis-ferrocenylethynyl-4, 4′-bipyridine (**103**) bearing two ferrocenylethynyl units linked to an axially chiral core on polysaccharide-based chiral columns, comparing these results to those of the analyte featuring the same structural motif

Table 7
Representative enantioseparations of chiral metal complexes reported in the 2010s.

Analyte	Metal	Compound type	Chiral column or selector[b]	Mobile phase[c]	Ref.
64	Au	$Au_{38}(SCH_2CH_2Ph)_{24}$	Lux Cellulose-1	*n*-hexane/2-PrOH 80:20 v/v	[53]
65	Au	$Au_{40}(SCH_2CH_2Ph)_{24}$	Lux Cellulose-1	*n*-hexane/2-PrOH 90:10 v/v	[55]
66	Au	$Au_{28}(TBBT^a)_{20}$	Lux Cellulose-1	*n*-hexane/2-PrOH 80:20 v/v	[56]
67	Os	Osmabenzene complex	Home-made β-CD-based CSP	EtOH (NH_4NO_3 (0.05 mol L^{-1})	[57]
68-88	Ru	Polypyridyl complexes	Cyclofructan-based CSPs	ACN/MeOH-based mixtures	[58]
89	Fe, Ru	Helicene metallocenes	Chiralpak IF	*n*-hexane/dichloromethane 3:1	[59]
90, 91	Rh, Ir	Octahedral complexes	Chiralpak IB	ACN/H_2O 65:35 (0.1 % AA)	[60]
92	Ir	Chiral-at metal complex	Chiralpak IB	ACN/H_2O 50:50 (0.1 % TFA)	[61]
93	Ir	Cage compound	Cyclofructan-based CSPs	methanol	[62]

[a] TBBT = 4-tert-butylbenzenethiolate.
[b] CD, cyclodextrin.
[c] AA, acetic acid; ACN, acetonitrile; EtOH, ethanol; MeOH, methanol; TFA, trifluoroacetic acid.

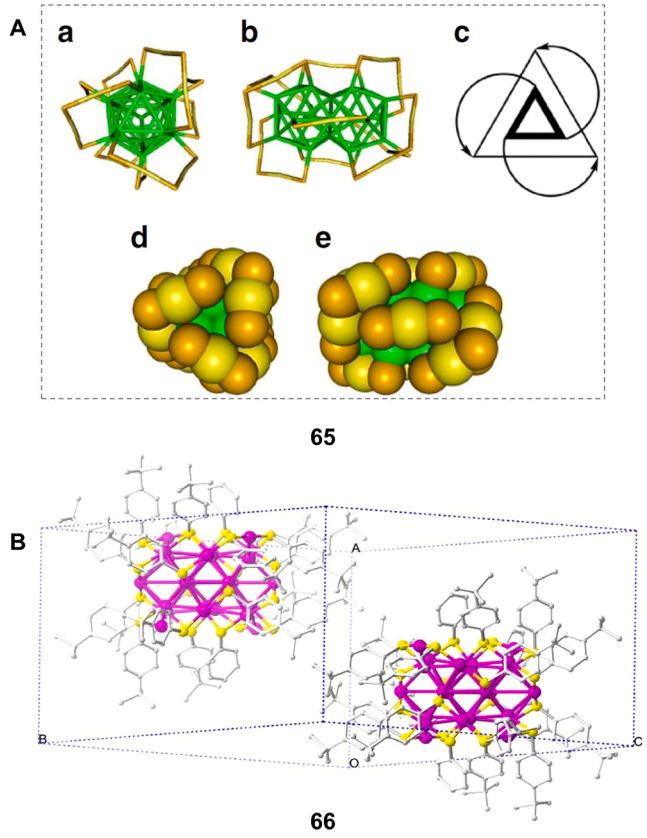

Fig. 10. (A) Crystal structure of the left-handed enantiomer of $Au_{38}(SCH_2CH_2Ph)_{24}$ (**65**). For clarity, the -CH_2CH_2Ph units is not shown. Colour legend: yellow, gold adatoms; green, core atoms (Au); orange, sulphur. (a) Top view of the cluster; (b) side-view; (c) schematic representation highlighting the handedness of the cluster. The inner triangle represents the top three core atoms binding to the long staples. The arrows represent long staples and the outer triangle represent the core Au atoms binding to the 'end' of the staple. This representation is a top view along the C_3 axis, and the two triangles are not in one plane. (d) Top-view in space-filling representation mode; (e) side-view in space-filling representation mode. Reproduced with permission from Ref. [53]. (B) Total structure of the $Au_{28}(TBBT)_{20}$ nanocluster (**66**). The unit cell contains a pair of left- and right-handed isomers. Colour legend: magenta = Au atoms; yellow = sulfur; grey = carbon. Reproduced with permission from Ref. [56]. (For interpretation of the references to color in this figure legend, the reader is referred to the web version of this article.)

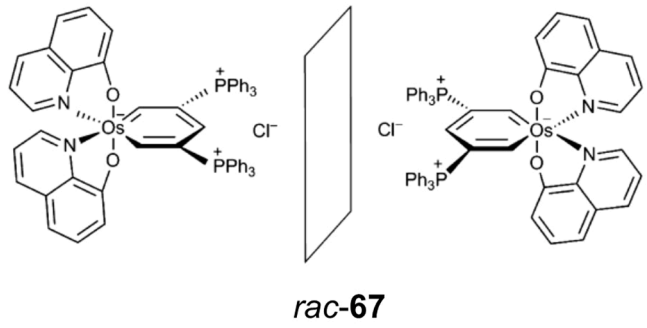

Fig. 11. Structure of the enantiomers of the osmabenzene **67**. Reproduced with permission from Ref. [57].

with two phenyl groups in place of the ferrocenyl moieties. The results of this study showed the superiority of the ferrocenyl compared to the phenyl group, as a structural element favouring enantiodifferentiation [71]. The collected data were reasonably consistent with a picture of the enantioselective recognition based on the interplay between HBs, π-π stacking and dispersion interactions dependent on analyte structure and features of the polysaccharide surfaces. In 2024, Grecchi *et al.* used *N, N*-dimethyl-1-ferrocenylethylamine (**104**) as test probes to examine the enantioseparation capability of wirelessly activated hollow tubular systems for the effective, simple, and tunable separation of racemic and enantioenriched mixtures [72,73]. These double-layered tubular objects consisted of an external polypyrrole chassis, a polymer with good electromechanical properties, functionalized in its inner part with an inherently chiral oligomer. The functioning of this system based on the synergy between the electromechanical pumping process of the outer layer and the enantioselective affinity of the inner part induces the system to behave as a miniaturized chiral column.

Although methods to enantioseparate ruthenium and osmium complexes were developed already in the past decades, in 2020s Armstrong's group developed interesting methods for the enantioseparation of chiral metal complexes of pharmaceutical interest. In 2021, five chiral Ru(II) and Os(II) polypyridyl complexes (**105-109**) (Fig. 17) were synthesized and their enantiomers separated for the first time [74]. Complex **105** had provided promising results as a photodynamic therapy agent for some types of cancer and is currently in Phase 2 clinical trials [75]. Both analytical and preparative chromatographic separations of all five racemates were developed using a derivatized cyclofructan (CF6-RN)-based chiral column under polar organic elution mode. The absolute configuration of the eluted compounds was determined using vibrational circular dichroism. In all cases, the first eluted peak was the Δ enantiomer and the second eluted peak was the Λ enantiomer. In 2022, cyclofructan-6 (CF6) derivatized with (*R*)-naphthyl ethyl groups was used by Armstrong's group for the first separation of the Δ- and Λ-enantiomers of 23 ionic octahedral polypyridyl Ru(II)-and Os (II)-complexes like **110** and **111** (Fig. 18) under SFC conditions. In this study, enantioselectivity on the CF6-based chiral column was shown to be dependent on the conjugation level and rigidity of the metal complexes [76].

6. Conclusions

In this review, we examined the evolution over time of methods and strategies used to separate the enantiomers of chiral organometallics and metal complexes at analytical and semipreparative level by enantioselective liquid chromatography. The use of HPLC has dominated the scenario in this field, whereas SFC methods were developed to a lesser degree. On the other hand, for metallocenes [70] and an heteroleptic Ir (III) complex [52] successful enantioseparations could be obtained with polysaccharide-based chiral columns in SFC, as well as with cyclofructans-based chiral columns for polypyridyl Ru(II) complexes [76]. Whereas in the 1990s, most enantioseparations were performed by using cellulose-based chiral columns with *n*-hexane-based mixtures as mobile phases, in the next decades the availability of multiple chiral columns on the market allowed to tackle method development by using and comparing chiral columns with different selectivity under different elution modes. Furthermore, the availability of immobilized polysaccharide-based chiral columns made using nonstandard solvents as components of the mobile phases possible and helpful. While, in some cases, *n*-hexane-based mobile phases were preferred for preparative-scale separations because removing organic solvents from the purified fractions is less energy-demanding compared to aqueous solutions [36,37], the use of polar organic and aqueous organic mobile phases resulted suitable for enantioselective LC-MS analysis in case of analysis of metal complexes of pharmaceutical and biomedical interest.

In the last decade, advancements in molecular design strategies, often supported by molecular modelling and computational analysis, have paved the way for new chiral metal complexes and metal clusters. On one hand, when the solubility of the chiral compounds enables the use of normal phase for their enantioseparation, methods based on the use of cellulose *tris*(3,5-dimethylphenylcarbamate)-based chiral

Table 8
Optimized enantiomeric separations of 21 ruthenium (II) polypyridyl complexes on LARIHC CF6-RN and LARIHC CF7-DMP.

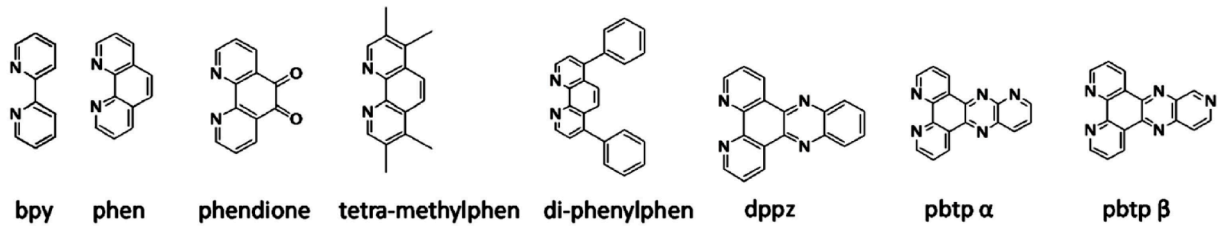

			LARIHC CF6-RN			LARIHC CF7-DMP		
N.	Name	Mobile phase[a]	k^b	α^c	$R_S{}^d$	k^b	α^c	$R_S{}^d$
68	$[Ru(phen)_2(phendione)](Cl_2)$	MeOH/AA/TEA 100:1.6:2.4	2.50	1.30	2.3	1.44	1.14	1.6
69	$[Ru(bpy)_2(phendione)](Cl_2)$	MeOH/AA/TEA 100:1.6:2.4	1.31	1.08	0.6	0.82	1.30	2.2
70	$[Ru(di\text{-}phenylphen)_2(phendione)](Cl_2)$	MeOH/AA/TEA 100:1.6:2.4	1.00	1.21	2.5	0.51	1.24	3.0
71	$[Ru(phen)_2(pbtp\ \beta)](PF_6)_2$	MeOH/ACN/$N(CH_3)_4NO_3$ 95:5:0.05	1.27	1.54	2.2	3.35	1.25	3.9
72	$[Ru(phen)_2(pbtp\ \alpha)](PF_6)_2$	MeOH/ACN/$N(CH_3)_4NO_3$ 95:5:0.05	1.31	1.50	3.0	3.10	1.26	4.2
73	$[Ru(phen)_2(dppz)](PF_6)_2$	ACN/MeOH/AA/TEA 30:70:1.6:4	4.52	1.53	3.7	2.37	1.25	4.4
74	$[Ru(phen)_2(p\text{-}CN\text{-}dppz)](PF_6)_2$	ACN/MeOH/AA/TEA 30:70:1.6:4	4.28	1.87	5.5	3.38	1.19	3.0
75	$[Ru(phen)_2(o\text{-}CN\text{-}dppz)](PF_6)_2$	ACN/MeOH/AA/TEA 30:70:1.6:4	5.38	1.44	3.1	3.08	1.21	3.3
76	$[Ru(phen)_2(p\text{-}Br\text{-}dppz)](PF_6)_2$	ACN/MeOH/AA/TEA 30:70:1.6:4	5.17	2.00	6.2	4.23	1.24	3.5
77	$[Ru(phen)_2(o\text{-}Br\text{-}dppz)](PF_6)_2$	ACN/MeOH/AA/TEA 30:70:1.6:4	5.55	1.59	4.0	3.60	1.27	3.6
78	$[Ru(phen)_2(o\text{-}F\text{-}dppz)](PF_6)_2$	ACN/MeOH/AA/TEA 30:70:1.6:4	4.24	1.53	3.3	2.42	1.25	3.3
79	$[Ru(phen)_2(o\text{-}Cl\text{-}dppz)](PF_6)_2$	ACN/MeOH/AA/TEA 30:70:1.6:4	4.38	1.54	3.9	3.43	1.26	4.0
80	$[Ru(Phen)_2(o\text{-}OCH_3\text{-}dppz)](PF_6)_2$	ACN/MeOH/AA/TEA 30:70:1.6:4	4.59	1.51	3.7	2.30	1.20	3.2
81	$[Ru(bpy)_2(o\text{-}OCH_3\text{-}dppz)](PF_6)_2$	ACN/MeOH/AA/TEA 30:70:1.6:4	4.58	1.23	1.8	1.59	1.11	1.9
82	$[Ru(bpy)_2(o\text{-}F\text{-}dppz)](PF_6)_2$	ACN/MeOH/AA/TEA 30:70:1.6:4	3.97	1.23	1.5	2.11	1.17	2.5
83	$[Ru(bpy)_2(o\text{-}Cl\text{-}dppz)](PF6)2$	ACN/MeOH/AA/TEA 30:70:1.6:4	4.10	1.24	1.7	3.72	1.18	3.1
84	$[Ru(bpy)_3](PF_6)_2$	MeOH/AA/TEA 100:1.6:4	6.79	1.06	0.6	1.44	1.04	0.5
85	$[Ru(phen)(bpy)_2](PF_6)_2$	MeOH/AA/TEA 100:1.6:4	7.86	1.12	1.0	2.52	1.07	0.8
86	$[Ru(phen)_2(bpy)](PF_6)_2$	MeOH/AA/TEA 100:1.6:4	8.44	1.22	1.9	2.88	1.13	1.5
87	$[Ru(di\text{-}phenylphen)_3](PF_6)_2$	MeOH/AA/TEA 100:1.6:4	0.86	1.56	1.9	1.57	1.06	1.0
88	$[Ru(tetra\text{-}methlyphen)_3](PF_6)_2$	MeOH/AA/TEA 100:1.6:4	1.24	2.28	4.3	2.27	1.20	0.9

[a] Numbers represent the volume ratio (v/v/v or v/v/v/v) of solvents (additives) in the mobile phase; AA, acetic acid; ACN, acetonitrile; MeOH, methanol; TEA, triethylamine.
[b] k = retention factor.
[c] α = selectivity factor.
[d] R_S = resolution factor.

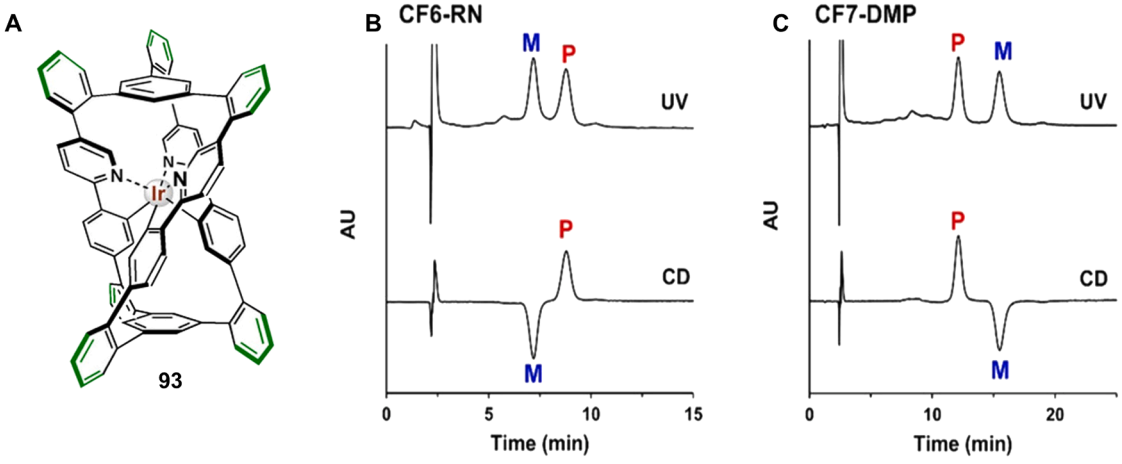

Fig. 12. (A) Structure of Ir-cage complex **93**. (B,C) Enantioselective HPLC chromatograms for **93** using the derivatized cyclofructan CSPs: CF6-RN (*R*-naphthylethyl derivatized cyclofructan-6) and CF7-DMP (3,5-dimethylphenyl derivatized cyclofructan-7). Adapted with permission from Ref. [62]. (For interpretation of the references to color in this figure legend, the reader is referred to the web version of this article.)

columns with *n*-hexane-containing mobile phases remain the most popular choice. For instance, the enantioseparation of Au-metal clusters is currently performed by using Lux Cellulose-1 under normal phase [77] exclusively, based on the same method developed in the 2010s by Dolamic *et al.* [53]. Differently, the enantioseparation of the first Ir-containing cage compound could not be achieved in normal phase due to the insolubility of the chiral cage in organic nonpolar solvents. In this case, the use of MeOH as polar organic solvent enabled the enantioseparation with a cyclofructan-based chiral column [62].

Although polysaccharide-based chiral columns remain the most applied for the enantioseparation of metal complexes by liquid chromatography, it is worth mentioning that β-CD-based chiral columns were also successfully applied with aqueous methanol for the enantioseparation of chiral ferrocenes, whereas cyclofructan- and glycopeptide-

Table 9
Representative enantioseparations of chiral metal complexes reported in the 2020s.

Analyte	Metal	Compound type	Chiral column or selector[a]	Mobile phase[b]	Ref.
94	Re	Tricarbonyl bipyridyl complex	Chiralpak IE	*n*-hexane/EtOH/TFA/DEA 60:40:0.1:0.1	[63]
95, 96	B	Bis(carbollide)s and carboranes	β-CD-based CSPs	MeOH/EDTA, MeOH/ACN/EDTA	[64]
95, 96	B	Bis(carbollide)s and carboranes	Polysaccharide CSPs	Aqueous-organic mixtures	[67]
96, 97	B,Co	Bis(carbollide)s	hydroxypropylated β-CD	Polar organic elution mode	[68]
98	B	Bis-aryl carbazole borane	Chiralpak AD-H	*n*-hexane/2-PrOH 97:3	[69]
99-102	Fe,Ru	Metallocenes	Polysaccharide CSPs	SFC	[70]
103	Fe	Ferrocene	Polysaccharide CSPs	Multimodal elution	[71]
104	Fe	Ferrocene	Inherently chiral oligomer	No solvent	[72]
105-109	Ru,Os	Polypyridyl complexes	Cyclofructan-based CSP	Polar organic elution mode	[74]
110, 111	Ru,Os	Polypyridyl complexes	Cyclofructan-based CSP	SFC	[76]

[a] CD, cyclodextrin.
[b] AA, acetic acid; ACN, acetonitrile; DEA, diethylamine; EDTA, ethylendiaminoacetic acid; EtOH, ethanol; MeOH, methanol; 2-PrOH, 2-propanol; SFC, supercritical fluid chromatography; TFA, trifluoroacetic acid.

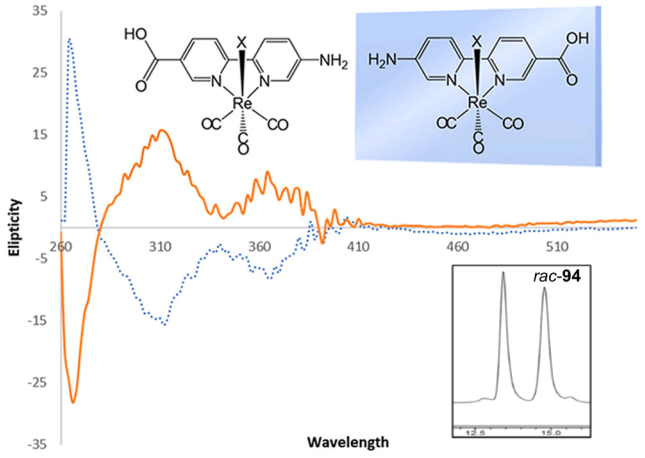

Fig. 13. Enantioselective HPLC chromatographic separation of compound **94** (X = Cl) (inset); circular dichroism spectroscopy of the two enantiomers of **94** carried out in DMF. Adapted with permission from Ref. [63]. (For interpretation of the references to color in this figure legend, the reader is referred to the web version of this article.)

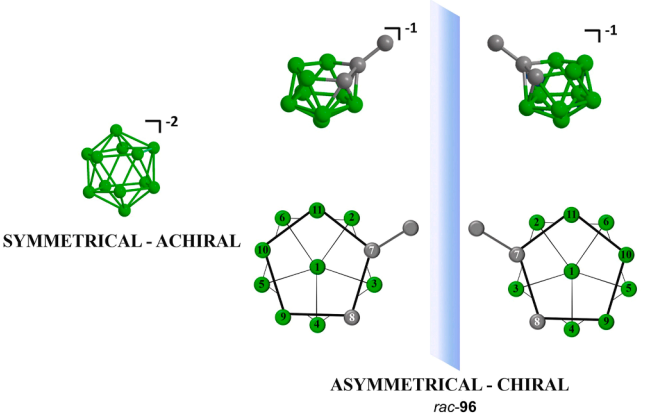

Fig. 14. The chirality of the [7-Me-*nido*-7,8-$C_2B_9H_{11}$]$^-$ anion **96** asymetrically substituted at one of the skeletal carbon atoms (C_s symmetry) in contrast with the highly symmetrical structure of dodecaborate anion $[B_{12}H_{12}]^{2-}$ (Point Group I_h). Reproduced with permission from Ref. [64]. (For interpretation of the references to color in this figure legend, the reader is referred to the web version of this article.)

based chiral columns proved to be suitable for the enantioseparation of polypyridyl Ru(II) complexes with acetonitrile/MeOH and reversed-phase mobile phases, respectively.

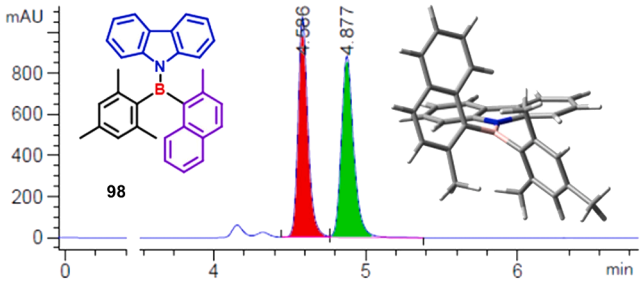

Fig. 15. Chromatographic trace of the HPLC enantioseparation of compound **98** on Chiralpak AD-H with *n*-hexane/2-PrOH 97:3 v/v, flow rate = 0.7 mL/min. Reproduced with permission from Ref. [69]. (For interpretation of the references to color in this figure legend, the reader is referred to the web version of this article.)

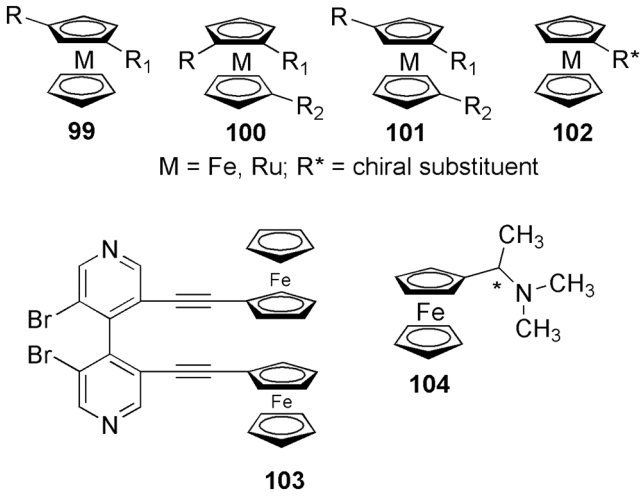

Fig. 16. Structures of chiral ferrocenes **99-104**.

CRediT authorship contribution statement

Barbara Sechi: Writing – review & editing, Data curation. **Sergio Cossu:** Writing – review & editing, Data curation. **Paola Peluso:** Writing – review & editing, Writing – original draft, Conceptualization.

Declaration of competing interest

The authors declare that they have no known competing financial interests or personal relationships that could have appeared to influence the work reported in this paper.

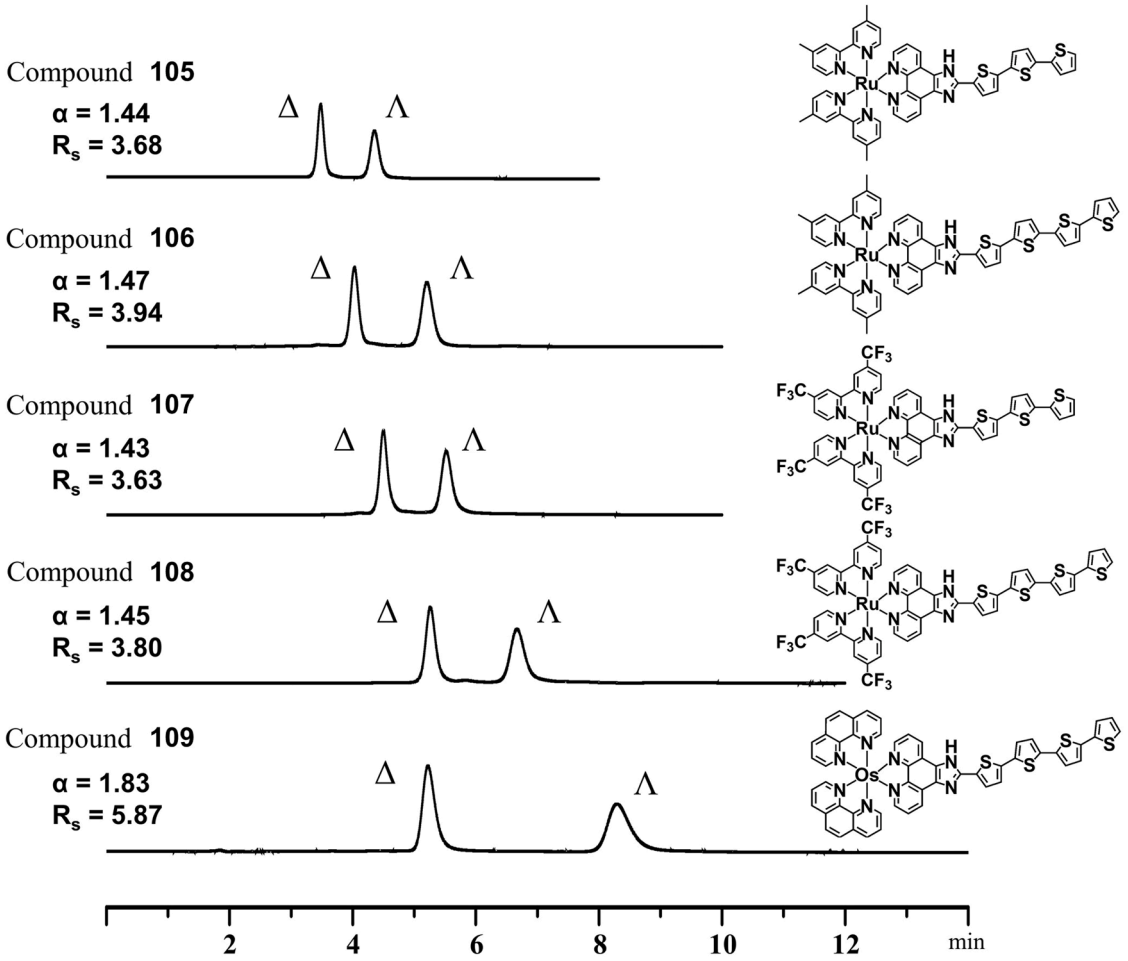

Fig. 17. Optimized enantiomeric separations of Ru and Os transition metal compounds **105-109** on the LARIHC CF6-RN column. Adapted with permission from Ref. [74].

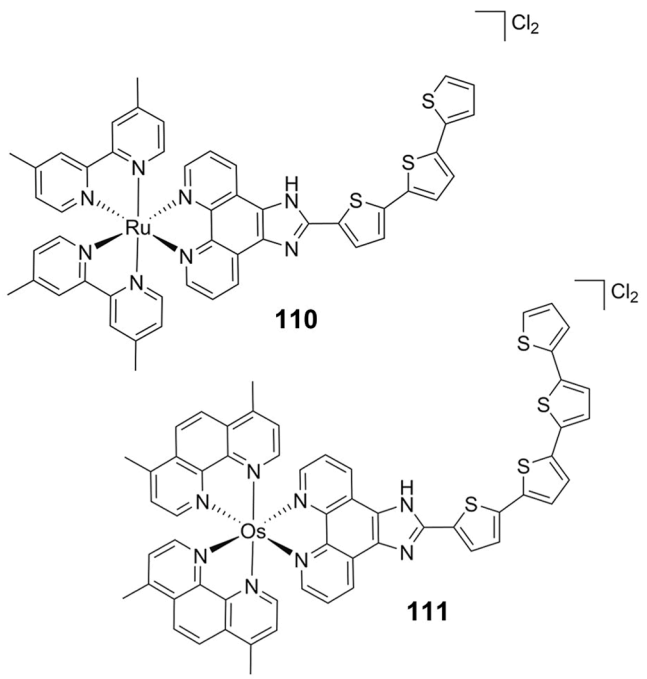

Fig. 18. Structures of ionic octahedral polypyridyl Ru(II)-and Os(II)-complexes **110** and **111**. Adapted with permission from Ref. [76].

Acknowledgements

We thank CNR for financial support.

References

[1] J. Karges, R.W. Stokes, S.M. Cohen, Metal complexes for therapeutic applications, Trends Chem. 3 (2021) 523–534, https://doi.org/10.1016/j.trechm.2021.03.006.
[2] P.S. Steinlandt, L. Zhang, E. Meggers, Metal stereogenicity in asymmetric transition metal catalysis, Chem. Rev. 123 (2023) 4764–4794, https://doi.org/10.1021/acs.chemrev.2c00724.
[3] R.H. Elattar, S.F. El-Malla, A.H. Kamal, F.R. Mansour, Applications of metal complexes in analytical chemistry: a review article, Coord. Chem. Rev. 501 (2024) 215568, https://doi.org/10.1016/j.ccr.2023.215568.
[4] P. Peluso, B. Sechi, G. Jibuti, Enantioseparation of organometallic compounds by electromigration techniques, Electrophoresis 45 (2024) 1018–1032, https://doi.org/10.1002/elps.202300231.
[5] Z.–H. Yan, D. Li, X.-B. Yin, Review for chiral-at-metal complexes and metal-organic framework enantiomorphs, Sci. Bull. 62 (2017) 1344–1354, https://doi.org/10.1016/j.scib.2017.09.013.
[6] J.B. Thomson, Molecular asymmetry in the ferrocene series, Tetrahedron Lett. 6 (1959) 26–27, https://doi.org/10.1016/S0040-4039(01)99425-0.
[7] H. Krebs, J. Diewald, H. Arlitt, J.A. Wagner, Über die chromatographische Spaltung von Racematen. II. Versuche zur Aktivierung von oktaederförmig gebauten Komplexen, Z. Anorg. U. Aligem. Chem. 287 (1956) 98–105, https://doi.org/10.1002/zaac.19562870115.
[8] T. Moeller, E. Gulyas, The partial resolution of certain inner complexes by means of a chromatographic technique, J. Inorg. Nucl. Chem. 5 (1958) 245–248, https://doi.org/10.1016/0022-1902(58)80138-4.
[9] H. Veening, J.M. Greenwood, W.H. Shanks, B.R. Willeford, Liquid chromatography of some arene tricarbonylchromium complexes, J. Chem. Soc. D: Chem. Commun. (1969) 1305, https://doi.org/10.1039/C2969001305A.

[10] K. Schlögl, Configurational and conformational studies in the metallocene field, Pure Appl. Chem. 23 (1970) 413–432, https://doi.org/10.1351/pac197023040413.

[11] H. Yoneda, T. Yoshizawa, Chromatography study of optical resolution I. Complete resolution of the neutral complex, facial isomer of tris (β-alaninato) cobalt (III), Chem. Lett. 7 (1976) 707–710, https://doi.org/10.1246/CL.1976.707.

[12] D.W. Armstrong, W. Demond, B.P. Czech, Separation of metallocene enantiomers by liquid chromatography: chiral recognition via cyclodextrin bonded phases, Anal. Chem. 57 (1985) 481–484, https://doi.org/10.1021/ac50001a037.

[13] Y. Okamoto, M. Kawashima, T. Hatada, Chromatographic resolution. XI. Controlled chiral recognition of cellulose triphenylcarbamate derivatives supported on silica gel, J. Chromatogr. A 63 (1986) 173–186, https://doi.org/10.1016/S0021-9673(01)83736-5.

[14] Y. Okamoto, E. Yashima, Polysaccharide derivatives for chromatographic separation of enantiomers, Angew. Chem. Int. Ed. 37 (1998) 1020–1043, https://doi.org/10.1002/(SICI)1521-3773(19980504)37:8<1020::AID-ANIE1020>3.0.CO;2-5.

[15] R. Aburatani, Y. Okamoto, K. Hatada, Optical resolving ability of 3,5-dimethylphenylcarbamates of oligosaccharides and cyclodextrins, Bull. Chem. Soc. Jpn. 63 (1990) 3606–3610, https://doi.org/10.1246/bcsj.63.3606.

[16] P. Peluso, V. Mamane, Ferrocene derivatives with planar chirality and their enantioseparation by liquid-phase techniques, Electrophoresis 44 (2023) 158–189, https://doi.org/10.1002/elps.202200148.

[17] J.A. Ramsden, C.M. Garner, J.A. Gladysz, Facile separations of enantiomers of chiral organometallic compounds with a Bakerbond Chiralcel HPLC column, Organometallics 10 (1991) 1631–1633, https://doi.org/10.1021/om00051a066.

[18] Y. Yamazaki, N. Morohashi, K. Hosono, High-performance liquid chromatographic determination of optical purity of planar chiral organometallic compounds resolved by enzymic transformations, J. Chromatogr. 542 (1991) 129–136, https://doi.org/10.1016/S0021-9673(01)88753-7.

[19] C. Villani, W.H. Pirkle, Direct high-performance liquid chromatographic resolution of planar chiral tricarbonyl (η^6-arene)-chromium (0) complexes, J. Chromatogr. A 693 (1995) 63–68, https://doi.org/10.1016/0021-9673(94)01041-C.

[20] S. Habaue, H. Sakamoto, Y. Okamoto, Optical resolution of chiral ethylenebis (4,5,6,7-tetrahydro-1-indenyl)zirconium derivatives by high-performance liquid chromatography, Chem. Lett. 25 (1996) 383–384, https://doi.org/10.1246/cl.1996.383.

[21] S. Habaue, H. Sakamoto, Y. Okamoto, Chiral ethylenebis(4,5,6, 7-tetrahydro-1-indenyl)zirconium 2,2'-biphenolate. Separation and application to asymmetric polymerization, Pol. J. 29 (1997) 384–386, https://doi.org/10.1295/polymj.29.384.

[22] T. Shimizu, M. Kobayashi, Optically Active selenoxides: chromatographic separation and absolute configuration, J. Org. Chem. 52 (1987) 3399–3403, https://doi.org/10.1021/jo00391a043.

[23] T. Shimizu, Y. Yamazaki, H. Taka, N. Kamigata, Isolation, stereochemistry, and configurational lability of optically active telluroxides, J. Am. Chem. Soc. 119 (1997) 5966–5967, https://doi.org/10.1021/ja970760i.

[24] M. Yoshifuji, Y. Ichigawa, K. Toyota, E. Kasashima, Y. Okamoto, Rotational isomers of a 1,2-diphenyl-3,4-diphosphinidenecyclobutene, Chem. Lett. 26 (1997) 87–88, https://doi.org/10.1246/cl.1997.87.

[25] O. Riant, G. Argouarch, D. Guillaneux, O. Samuel, H. Kagan, A straightforward asymmetric synthesis of enantiopure 1,2- disubstituted ferrocenes, J. Org. Chem. 63 (1998) 3511–3514, https://doi.org/10.1021/jo9800614.

[26] L.V. Snegur, V.I. Boev, Y.S. Nekrasov, M.M. Ilyin, V.A. Davankov, Z.A. Starikova, A. I. Yanovsky, A.F. Kolomiets, V.N. Babin, Synthesis and structure of biologically active ferrocenylalkyl polyfluoro benzimidazoles, J. Organomet. Chem. 580 (1999) 26–35, https://doi.org/10.1016/S0022-328X(98)01097-3.

[27] Y. Kaida, Y. Okamoto, The separation of optically active copper(I) catenates, Tetrahedron Lett. 34 (1993) 1019–1022, https://doi.org/10.1016/S0040-4039(00)77481-8.

[28] T. Mizutani, T. Ema, T. Tomita, Y. Kuroda, H. Ogoshi, Design and synthesis of a trifunctional chiral porphyrin with C2 symmetry as a chiral recognition host for amino acid esters, J. Am. Chem. Soc. 116 (1994) 4240–4250, https://doi.org/10.1021/ja00089a013.

[29] K. Tashiro, K. Konishi, T. Aida, Enantiomeric resolution of chiral metallobis (porphyrin)s: studies on rotatability of electronically coupled porphyrin ligands, Angew. Chem. Int. Ed. Engl. 36 (1997) 856–858, https://doi.org/10.1002/anie.199708561.

[30] A. Werner, M. Michels, L. Zander, J. Lex, E. Vogel, Figure Eight" cyclooctapyrroles: enantiomeric separation and determination of the absolute configuration of a binuclear metal complex, Angew. Chem. Int. Ed. 38 (1999) 3650–3653, https://doi.org/10.1002/(SICI)1521-3773(19991216)38:24<3650::AID-ANIE3650>3.0.CO;2-F.

[31] B. Grüner, J. Holub, J. Plešek, T. Vaněk, H. Votavová, High-performance liquid chromatographic enantiomeric resolution in the ten-vertex carborane series comparison of acetyl- and native β-cyclodextrin bonded chiral stationary phases, J. Chromatogr. A 793 (1998) 249–256, https://doi.org/10.1016/S0021-9673(97)00904-7.

[32] D.W. Armstrong, J.T. Lee, L.W. Chang, Enantiomeric impurities in chiral catalysts, auxiliaries and synthons used in enantioselective synthesis, Tetrahedron: Asymmetry 9 (1998) 2043–2064, https://doi.org/10.1016/S0957-4166(98)00201-8.

[33] J. Zukowski, Determination of the enantiomeric purity of commercial Jacobsen's catalyst samples, Chirality 10 (1998) 362–363, https://doi.org/10.1002/(SICI)1520-636X(1998)10:4<362::AID-CHIR12>3.0.CO;2-Y.

[34] H. Qiu, N.L.T. Padivitage, L.A. Frink, D.W. Armstrong, Enantiomeric impurities in chiral catalysts, auxiliaries, and synthons used in enantioselective syntheses. Part 4, Tetrahedron: Asymmetry 24 (2013) 1134–1141, https://doi.org/10.1016/j.tetasy.2013.07.019.

[35] N. Thakur, R.A. Patil, M. Talebi, E.R. Readel, D.W. Armstrong, Enantiomeric impurities in chiral catalysts, auxiliaries, and synthons used in enantioselective syntheses. Part 5, Chirality 31 (2019) 688–699, https://doi.org/10.1002/chir.23086.

[36] J.C. Ruble, G.C. Fu, Chiral π-complexes of heterocycles with transition metals: a versatile new family of nucleophilic catalysts, J. Org. Chem. 61 (1996) 7230–7231, https://doi.org/10.1021/jo961433g.

[37] P.I. Dosa, J.C. Ruble, G.C. Fu, Planar-chiral heterocycles as ligands in metal-catalyzed processes: enantioselective addition of organozinc reagents to aldehydes, J. Org. Chem. 62 (1997) 444–445, https://doi.org/10.1021/jo962156g.

[38] F. Gasparrini, I. D'Acquarica, J.G. Vos, C.M. O'Connor, C. Villani, Efficient enantiorecognition of ruthenium(II) complexes by silica-bond teicoplanin, Tetrahedron: Asymmetry 11 (2000) 3535–3541, https://doi.org/10.1016/S0957-4166(00)00292-5.

[39] P. Sun, A. Krishnan, A. Yadav, S. Singh, F.M. MacDonnell, D.W. Armstrong, Enantiomeric separations of ruthenium(II) polypyridyl complexes using high-performance liquid chromatography (HPLC) with cyclodextrin chiral stationary phases (CSPs), Inorg. Chem. 46 (2007) 10312–10320, https://doi.org/10.1021/ic701023x.

[40] P. Sun, A. Krishnan, A. Yadav, F.M. MacDonnell, D.W. Armstrong, Enantioseparation of chiral ruthenium(II) polypyridyl complexes using HPLC with macrocyclic glycopeptide chiral stationary phases (CSPs), J. Mol. Struct. 890 (2008) 75–80, https://doi.org/10.1016/j.molstruc.2008.02.030.

[41] J.G. Hansen, M. Johannsen, Pentamethylated and pentaphenylated azaferro- and azaruthenocenes: simple and general methodology for the preparation of enantiopure derivatives, J. Org. Chem. 68 (2003) 1266–1274, https://doi.org/10.1021/jo026333r.

[42] A.A. Simenel, Y.V. Kuzmenko, E.A. Morozova, M.M. Ilyn, I.F. Gun'ko, L.V. Snegur, Synthesis and enantiomeric resolution of ferrocenyl(alkyl)azoles, J. Organomet. Chem. 688 (2003) 138–143, https://doi.org/10.1016/j.jorganchem.2003.08.039.

[43] A. Patti, S. Pedotti, C. Sanfilippo, Comparative HPLC enantioseparation of ferrocenylalcohols on two cellulose-based chiral stationary phases, Chirality 19 (2007) 344–351, https://doi.org/10.1002/chir.20386.

[44] B. Mayr, H. Schottenberger, O. Elsner, M.R. Buchmeiser, Separation of planar chiral ferrocene derivatives on β-cyclodextrin-based polymer supports prepared via ring-opening metathesis graft-polymerization, J. Chromatogr. A 973 (2002) 115–122, https://doi.org/10.1016/S0021-9673(02)01197-4.

[45] B. Sechi, A. Dessì, C. Gatti, R. Dallocchio, B. Chankvetadze, S. Cossu, V. Mamane, P. Pale, P. Peluso, Unravelling functions of halogen substituents in the enantioseparation of halogenated planar chiral ferrocenes on polysaccharide-based chiral stationary phases: experimental and electrostatic potential analyses, J. Chromatogr. A 1673 (2022) 463097, https://doi.org/10.1016/j.chroma.2022.463097.

[46] X.P. Chen, Z.M. Zhou, H. Yuan, Z.H. Meng, Preparation and chiral recognition of a novel chiral stationary phase for HPLC, based on mono(6^A-N-1-(2-hydroxyl)-phenylethylimino-6^A-deoxy)-β-cyclodextrin and covalently bonded silica gel, Chin. Chem. Lett. 19 (2008) 797–800, https://doi.org/10.1016/j.cclet.2008.04.045.

[47] X. Chen, Z. Zhou, H. Yuan, Z. Meng, Preparation and chiral recognition of a mono ((6^A-N-1-(2-hydroxy)-phenylethylimino-6^A-deoxy)-β-cyclodextrin HPLC stationary phase, J. Chromatogr. Sci. 46 (2008) 777–782, https://doi.org/10.1093/chromsci/46.9.777.

[48] X. Wang, W.Z. Li, Q.-Y. Zhao, Y.-M. Li, L.-R. Chen, Normal-phase HPLC enantioseparation of novel chiral metal tetrahedrane-type clusters on an amylose-based chiral stationary phase, Anal. Sci. 21 (2005) 125–128, https://doi.org/10.2116/analsci.21.125.

[49] T.E. Wood, N.D. Dalgleish, E.D. Power, A. Thompson, X. Chen, Y. Okamoto, Stereochemically stable double-helicate dinuclear complexes of bis (dipyrromethene)s: A chiroptical study, J. Am. Chem. Soc. 127 (2005) 5740–5741, https://doi.org/10.1021/ja0500613.

[50] M.M. Warnke, F.A. Cotton, D.W. Armstrong, Enantioseparation of extended metal atom chain complexes: unique compounds of extraordinarily high specific rotation, Chirality 19 (2007) 179–183, https://doi.org/10.1002/chir.20355.

[51] D.W. Armstrong, F.A. Cotton, A.G. Petrovic, P.L. Polavarapu, M.M. Warnke, Resolution of enantiomers in solution and determination of the chirality of extended metal atom chains, Inorg. Chem. 46 (2007) 1535–1537, https://doi.org/10.1021/ic062263l.

[52] F.J. Coughlin, M.S. Westrol, K.D. Oyler, N. Byrne, C. Kraml, E. Zysman-Colman, M. S. Lowry, S. Bernhard, Synthesis, separation, and circularly polarized luminescence studies of enantiomers of iridium(III) luminophores, Inorg. Chem. 47 (2008) 2039–2048, https://doi.org/10.1021/ic701747j.

[53] I. Dolamic, S. Knoppe, A. Dass, T. Bürgi, First enantioseparation and circular dichroism spectra of Au_{38} clusters protected by achiral ligands, Nat. Comm. 3 (2012) 1–6, https://doi.org/10.1038/ncomms1802.

[54] M.V. Mukhina, I.V. Korsakov, V.G. Maslov, F. Purcell-Milton, J. Govan, A. V. Baranov, A.V. Fedorov, Y.K. Gun'ko, Molecular recognition of biomolecules by chiral CdSe quantum dots, Sci. Rep. 6 (2016) 24177, https://doi.org/10.1038/srep24177.

[55] S. Knoppe, I. Dolamic, A. Dass, T. Bürgi, Separation of enantiomers and cd spectra of $Au_{40}(SCH_2CH_2Ph)_{24}$: spectroscopic evidence for intrinsic chirality, Angew. Chem. Int. Ed. 51 (2012) 7589–7591, https://doi.org/10.1002/anie.201202369.

[56] C. Zeng, T. Lao, A. Das, N.L. Rosi, R. Jin, Chiral structure of thiolate-protected 28-gold-atom nanocluster determined by X-ray crystallography, J. Am. Chem. Soc. 135 (2013) 10011–10013, https://doi.org/10.1021/ja404058q.
[57] C. Lin, W. Liu, J. Fan, Y. Wang, S. Zheng, R. Lin, H. Zhang, W. Zhang, Synthesis of a novel cyclodextrin-derived chiral stationary phase with multiple urea linkages and enantioseparation toward chiral osmabenzene complex, J. Chromatogr. A 1283 (2013) 68–74, https://doi.org/10.1016/j.chroma.2013.01.087.
[58] Y. Shu, Z.S. Breitbach, M.K. Dissanayake, S. Perera, J.M. Aslan, N. Alatrash, F. M. MacDonnell, D.W. Armstrong, Enantiomeric separation of Ruthenium (II) polypyridyl complexes using HPLC with cyclofructan chiral stationary phases, Chirality 27 (2015) 64–70, https://doi.org/10.1002/chir.22389.
[59] M. Akiyama, K. Nozaki, Synthesis of optically pure helicene metallocenes, Angew. Chemie Int. Ed. 56 (2017) 2040–2044, https://doi.org/10.1002/anie.201611488.
[60] M. Carmona, R. Rodríguez, V. Passarelli, F.J. Lahoz, P. García-Orduña, D. Carmona, Metal as source of chirality in octahedral complexes with tripodal tetradentate ligands, J. Am. Chem. Soc. 140 (2018) 912–915, https://doi.org/10.1021/jacs.7b12731.
[61] Y. Tan, K. Harms, E. Meggers, A chiral-at-metal iridium catalyst with two simple but sterically demanding cyclometalated *N*-heterocyclic carbene ligands, Eur. J. Inorg. Chem. 22 (2018) 2500–2504, https://doi.org/10.1002/ejic.201800450.
[62] H. Sato, M.A. Blemker, G. Hellinghausen, D.W. Armstrong, J.W. Nafie, S. T. Roberts, M.J. Krische, Triple helical Ir(ppy)$_3$ phenylene cage prepared by diol-mediated benzannulation: synthesis, resolution, absolute stereochemistry and photophysical properties, Chem. Eur. J. 25 (2019) 8719–8724, https://doi.org/10.1002/chem.201902122.
[63] S. Gaire, B.R. Schrage, C.J. Ziegler, An organometallic isostere of an amino acid, Inorg. Chem. 60 (2021) 10105–10108, https://doi.org/10.1021/acs.inorgchem.1c01444.
[64] O. Horáček, M. Papajová-Janetková, B. Grüner, L. Lochman, P. Štěrbová-Kovaříčová, R. Vespalec, R. Kučera, The first chiral HPLC separation of dicarba-*nido*-undercarbonate anions and their chromatographic behavior, Talanta 222 (2021) 121652, https://doi.org/10.1016/j.talanta.2020.121652.
[65] I. Fuentes, T. Garcia-Mendiola, S. Sato, M. Pita, H. Nakamura, E. Lorenzo, F. Teixidor, F. Marques, C. Vinas, Metallacarboranes on the road to anticancer therapies: cellular uptake, DNA interaction, and biological evaluation of cobaltabisdicarbollide COSAN (-), Chem. Eur J. 24 (65) (2018) 17239–17254, https://doi.org/10.1002/chem.201803178.
[66] D. Mangelings, Y. Vander Heyden, R. Vespalec, Chiral separability of boron cluster species studied by screening approaches utilizing polysaccharide-based chiral stationary phases, Biomed. Chromatogr. 28 (5) (2014) 694–707, https://doi.org/10.1002/bmc.3091.
[67] O. Horáček, J. Marvalová, K. Štilcova, J. Holub, B. Grüner, R. Kučera, Reversed-phase chromatography as an effective tool for the chiral separation of anionic and zwitterionic carboranes using polysaccharide-based chiral selectors, J. Chromatogr. A 1672 (2022) 463051, https://doi.org/10.1016/j.chroma.2022.463051.
[68] O. Horáček, U. Dhaubhadel, J. Holub, B. Grüner, D.W. Armstrong, R. Kučera, Employment of chiral columns with superficially porous particles in chiral separations of cobalt bis (dicarbollide) and *nido*-7,8-$C_2B_9H_{12}$(1-) derivatives, Chirality 35 (2023) 937–951, https://doi.org/10.1002/chir.23606.
[69] D. Pecorari, E. Giuliani, A. Mazzanti, S. Stagni, V. Fiorini, G. Vigarani, F. Zinna, G. Pescitelli, M. Mancinelli, Synthesis and stereodynamic and emission properties of dissymmetric bis-aryl carbazole boranes and identification of a CPL-active B-C atropisomeric compound, J. Org. Chem. 88 (2023) 871–881, https://doi.org/10.1021/acs.joc.2c02209.
[70] L. Bonin, A. Morvan, G. Coadou, C. Furman, E. Boulanger, A. Ghinet, E. Lipka, Supercritical fluid chromatography for separation of chiral planar metallocenes, J. Chromatogr. A 1674 (2022) 463115, https://doi.org/10.1016/j.chroma.2022.463115.
[71] B. Sechi, A. Dessì, R. Dallocchio, N. Tsetskhladze, B. Chankvetadze, M. Pérez-Baeza, S. Cossu, G. Jibuti, V. Mamane, P. Peluso, Unravelling dispersion forces in liquid-phase enantioseparation. Part I: Impact of ferrocenyl versus phenyl groups, Anal. Chim. Acta 1278 (2023) 341725, https://doi.org/10.1016/j.aca.2023.341725.
[72] S. Grecchi, F. Malacarne, R. Cirilli, M. Dell'Edera, S. Ghirardi, T. Benincori, S. Arnaboldi, Wireless hollow miniaturized objects for electro assisted chiral resolution, Anal. Chem. 96 (2024) 4901–4908, https://doi.org/10.1021/acs.analchem.3c05544.
[73] S. Grecchi, G. Salinas, R. Cirilli, T. Benincori, S. Ghirardi, A. Kuhn, S. Arnaboldi, Miniaturized enantioselective tubular devices for the electromechanical wireless separation of chiral analytes, Chem 10 (2024) 660–674, https://doi.org/10.1016/j.chempr.2023.11.001.
[74] D.W. Armstrong, J. Yu, H.D. Cole, S.A. McFarland, J. Nafie, Chiral resolution and absolute configuration determination of new metal-based photodynamic therapy antitumor agents, J. Pharm. Biomed. Anal. 204 (2021) 114233, https://doi.org/10.1016/j.jpba.2021.114233.
[75] S.A. McFarland, A. Mandel, R. Dumoulin-White, G. Gasser, Metal-based photosensitizers for photodynamic therapy: the future of multimodal oncology? Curr. Opin. Chem. Biol. 56 (2020) 23–27, https://doi.org/10.1016/j.cbpa.2019.10.004.
[76] T.T. Handlovic, M.F. Wahab, H.D. Cole, N. Alatrash, E. Ramasamy, F. M. MacDonnell, S.A. McFarland, D.W. Armstrong, Insights into enantioselective separations of ionic metal complexes by sub/supercritical fluid chromatography, Anal. Chim. Acta 1228 (2022) 340156, https://doi.org/10.1016/j.aca.2022.340156.
[77] V. Truttmann, A. Loxha, R. Banu, E. Pittenauer, S. Malola, M.F. Matus, Y. Wang, E. A. Ploetz, G. Rupprechter, T. Bürgi, H. Häkkinen, C. Aikens, N. Barrabés, Directing intrinsic chirality in gold nanoclusters: preferential formation of stable enantiopure clusters in high yield and experimentally unveiling the "super" chirality of Au_{144}, ACS Nano 17 (2023) 20376–20386, https://doi.org/10.1021/acsnano.3c06568.